SveBeFo

STIFTELSEN SVENSK BERGTEKNISK FORSKNING
SWEDISH ROCK ENGINEERING RESEARCH

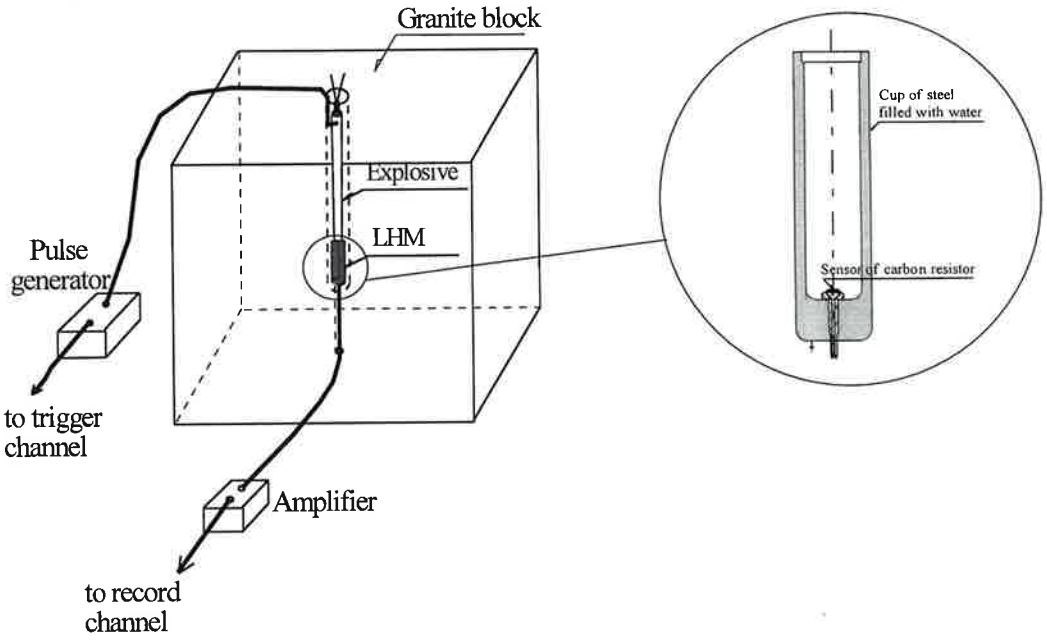

BOREHOLE PRESSURE IN BLAST HOLES
Measurements in granite blocks versus estimations

Shulin Nie

SveBeFo Report 42

STIFTELSEN SVENSK BERGTEKNISK FORSKNING
SWEDISH ROCK ENGINEERING RESEARCH

BOREHOLE PRESSURE IN BLAST HOLES - Measurements in granite blocks versus estimations

Borrhålstryck i sprängborrhål - mätning i stenblock och uppskattning

Shulin Nie

SveBeFo Report 42

Stockholm 1999
ISSN 1104-1773
ISRN SVEBEFO-R--42--SE

FÖRORD

I praktiska försök för att utveckla metoder för skonsam sprängning har det visat sig att sprängämnets kopplingsgrad är en viktig faktor, dvs hur stor del av borrhålsdiametern som upptas av sprängämne. Det är ett fenomen som kan utnyttjas för att förbättra sprängningstekniken men det förutsätter en bättre förståelse av vissa grundläggande samband mellan sprängämnens energiinnehåll och deras expansionsförmåga under olika förhållanden. För att korrelera teoretiska modeller med praktiska erfarenheter är tryck-förloppet vid detonationen en central fråga. En metod har därför tagits fram vid SveBeFo för att registrera dessa kortvariga, mycket höga tryck, upp till några GPa. I föreliggande rapport redovisas resultaten från sprängningar av enskilda borrhål i sten-block med registrering av de första 30 - 500 mikrosekunderna av förloppet med hjälp av den sk LHM-cellen. Överensstämmelsen med olika empiriska formler diskuteras och förslag till förbättringar av dessa görs. Ytterligare försök kommer att göras för att åstad-komma överensstämmelse mellan mätta och beräknade trycknivåer.

Resultaten är av stor betydelse i det pågående arbetet med att anpassa sprängämnen och hålsättning för ett effektivt och väl kontrollerat sprängningsresultat i olika praktiska till-lämpningar.

Projektet följs av SveBeFos "referensgrupp för detonik", under ordförandeskap av Stefan Lamnevik, FOA, och med representanter för Dyno Nobel och Kimit.

Stockholm i maj 1999

Tomas Franzén

SUMMARY

Borehole pressure is a measure of the expansion work an explosive can carry out in a blast hole. It is hence a fundamental parameter indicating energy partitioning and efficiency of the explosive. It is also the most important factor that determines the blasting results such as fragmentation, heave and damage in remaining rock. Recently, a method for measurement of pressure history in blast holes, the so-called LHM method, has been developed and successfully applied in laboratory tests. In order to extend the application of this new method to rock blasting, a series of measurements of borehole pressure using the LHM method have been conducted in blasting holes in large blocks of a very competent granite. Seven test shots have been carried out, in which two types of explosives and three decoupling ratios (borehole diameter/charge diameter) were studied. The experiments showed that the LHM method worked very well after minor modifications. The measured borehole pressure varied from 0.08 to 1.7 GPa, depending on the explosive type and decoupling ratio. However, only a part of the pressure history, 30 to 500 μs could be measured before the gage was damaged. The measured pressure amplitude has been used to calibrate empirical formulas. The calibration showed that the empirical formulas for explosion pressure provide quite good estimates while the formulas for borehole pressure in decoupled holes give poor estimates. However, when the decoupling ratio is large, approximately 2.4, Calder's formula can estimate the borehole pressure in decoupled holes well. Finally, a new estimation principle is proposed and a new formula based on this principle has been presented.

Keywords: borehole pressure, explosion pressure, decoupling, pressure gage, LHM

SAMMANFATTNING

Borrhålstryck är ett mått på sprängämnets expansionsförmåga i ett borrhål. Det är därför en grundläggande indikator på energifördelning och effektivt utnyttjande av sprängämne. Det är också en viktig faktor som avgör sprängresultat t ex fragmentering, kast och skador i kvarstående berg. En ny metod avsedd för mätning av borrhålstryck, den så kallade LHM (Lägesbestämd Hydrostatisk Mätkopp) metoden, har utvecklats och framgångsrikt använts i laboratorium. För att bredda metodens tillämpning till bergsprängning, har metoden använts för mätningar av borrhålstryck i detonerande borrhål i granitblock. Sju testskott sköts, där två sprängämnen och tre olika frikopplingar undersöktes. Försöken visade att LHM-metoden fungerade bra efter smärre modifikationer. Mätta borrhålstryck varierade mellan 0,08 och 1,7 GPa beroende på sprängämnestyp och frikopplingsgrad. Emellertid kunde bara delar av tryckförloppen, 30 till 500 μs mätas innan givaren förstördes. De uppmäta trycknivåerna har jämförts med empiriska uppskattningar. Jämförelsen visade att de empiriska formlerna för explosionstryck ger god överensstämmelse medan formlerna för borrhålstryck i frikopplat borrhål ger dålig överensstämmelse. I fallet där frikopplingen är stor med en frikopplingsgrad (håldiametern/laddningsdiametern) på 2,4 stämde Calder-formeln väl med mätningen. Slutligen har en ny beräkningsprincip föreslagits och motsvarande formel framtagits.

CONTENTS

1 INTRODUCTION

The history of the borehole pressure in a blast hole in rock describes the expansion work of the explosive during the rock breakage process. This data directly indicates the transfer of the explosive energy into the rock and hence it is a direct measure of the efficiency of the explosive. Furthermore, the borehole pressure determines the blasting results such as fragmentation, heave and damage in the remaining rock /1, 2, 3/. Besides, it is a crucial input or calibration data for various computer simulations. Therefore, this information is the most important one in an evaluation of the explosive performance and in the prediction of blasting results.

Despite of the importance of this parameter, direct measurements of the borehole pressure have rarely been carried out, owing to the absence of feasible methods. Instead, various empirical formulas or computer codes are used to estimate this pressure. The accuracy of such estimates remains unknown.

Recently, a method for measurement of pressure history in blast holes has been developed by G Persson at SveBeFo and successfully applied in laboratory tests /4/. The method has been named as LHM (In Swedish: Lägesbestämd Hydrostatisk Mätkopp, or Location-fixed Hydrostatic Measuring-cup) method /4/. In order to extend the application of this new method to rock blasting, a series of measurements of borehole pressure using the LHM method have been conducted in blasting holes in large blocks of very competent granite. The next step is to apply this method in field scale. More measurements in bench blasting are under way.

This report describes the borehole pressure measurements in blast holes in granite blocks using the LHM method. The comparison between the measured pressure amplitude and estimates by empirical formulas will be included.

1.1 Definition of the borehole pressure

The pressure inside a blast hole is a dynamic pressure. Different terms have been given to some specific moments in the pressure history, see Fig. 1 where the detonation pressure, explosion pressure and borehole pressure have been defined.

In a detonation, the unreacted explosive is first compressed to a higher density. As the reaction in the explosive starts and progresses, the reacting explosive expands and reaches the C-J plane or the sonic plane. The pressure at the C-J plane is defined as the detonation pressure /5/. At the C-J plane, the explosive has completely reacted in an ideal detonation, while in a non-ideal detonation, the reaction continues. After the C-J plane, the detonation products (in an ideal detonation) or the reacting explosive (in a non-ideal detonation) expands further and reaches the original volume of the explosive.

At this moment, the pressure inside the products or the reacting explosive is defined as the explosion pressure.

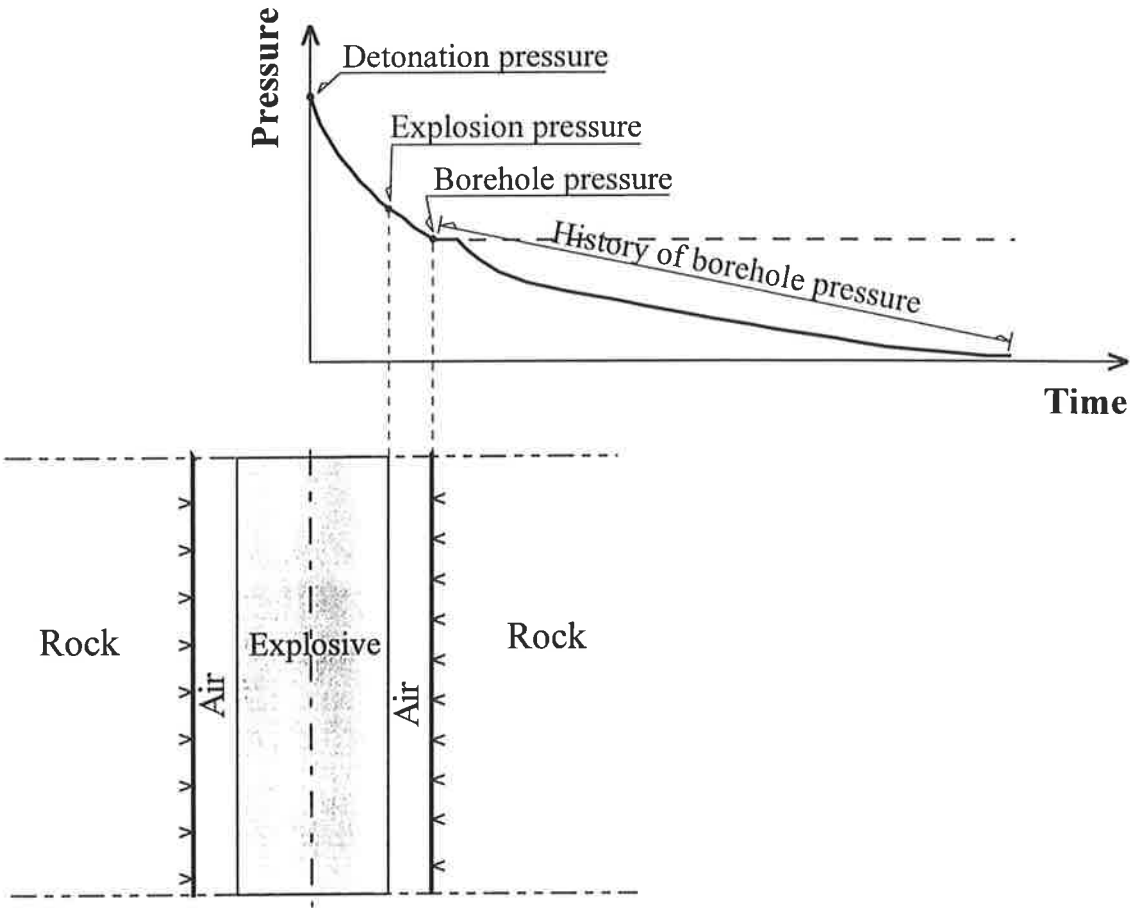

Fig. 1: Definitions of some specific pressures on the pressure history in a blasting hole.

The detonation pressure can be calculated by Eq. 1 /6/, whether the detonation is ideal or non-ideal (see Appendix I for the derivation of the formula):

$$P_{CJ} = \rho_0 D^2/(\gamma_{CJ}+1) \qquad (1)$$

where: P_{CJ} = detonation pressure (Pa)
ρ_0 = density of the explosive at the ambient state (kg/m^3)
D = velocity of detonation (m/s)
γ_{CJ} = adiabatic gamma at C-J plane = $-(\partial \ln P/\partial \ln v)_S$ at C-J plane
P = pressure (Pa)
v = volume (m^3) or specific volume (m^3/kg)

Furthermore, if the expansion from the C-J plane to the original explosive volume is assumed to obey the polytropic gas equation of state (EOS) or the γ-law EOS with a constant γ value, then the explosion pressure is exactly a half of the detonation pressure /6/, i.e.

$$P_e = \tfrac{1}{2}\cdot\rho_0 D^2/(\gamma_{CJ}+1) \qquad (2)$$

where: P_e = explosion pressure (Pa)

In the case that the explosive charge is de-coupled in a blast hole, the products or reacting explosive will expand to fill the whole blast hole. At this moment, yet before any expansion of the borehole wall has taken place, the pressure exerted on the blast hole wall is defined as the borehole pressure /5/. If the explosive completely fills a blast hole, i.e. no decoupling, the borehole pressure is the same as the explosion pressure.

Assuming that the expansion of the detonating explosive from the original explosive volume to the borehole volume a) is an isentropic process and b) obeys the polytropic gas equation of state (EOS) or the γ-law EOS with a constant γ value, then the relation between the borehole pressure in a fully charged blast hole, P_e, and in a decoupled blast hole, P_b, can be deduced, as described below.

$$\gamma = -\left(\frac{\partial \ln P}{\partial \ln v}\right)_s = \text{constant} \qquad (3)$$

can be transformed to

$$Pv^{\gamma} = \text{constant} \qquad (4)$$

Applying to the expansion from P_e to P_b in a blast hole:

$$P_e v_e^{\gamma} = P_b v_b^{\gamma} \qquad (5)$$

That is:

$$P_b = P_e \cdot \left(\sqrt{\frac{L_e}{L_b}} \cdot \frac{r_e}{r_b}\right)^{2\gamma} \qquad (6)$$

here: γ = adiabatic gamma
P = pressure (Pa)
v = volume (m^3)
S = entropy (J)
P_e = explosion pressure or borehole pressure in the fully charged blast hole (Pa)
v_e = volume of the explosive (m^3)
P_b = borehole pressure in the decoupled blast hole (Pa)
v_b = volume of the borehole (m^3)
L_e = length of the charge (m)
L_b = length of the borehole (m)
r_e = radius of the charge (m)
r_b = radius of the borehole (m)

As the blast hole expands, the pressure on the wall decreases and finally reaches the ambient pressure. This decreasing pressure on the blast hole wall during the blast hole expansion is hence called the time history of borehole pressure. Should the blast hole wall be rigid and adiabatically isolated, the borehole pressure would remain constant and the history of borehole pressure be a straight line, like the broken line shown in Fig. 1.

In order to calculate the above-mentioned different pressures, Eqs. 1, 2 and 6 can be used. In these equations, the parameters of charging geometry, the explosive density and the VOD can be readily measured with good accuracy. Meanwhile, it is too difficult to directly measure the values for γ_{CJ} and γ. Therefore, empirical formulas for γ_{CJ} and γ have great engineering significance. That is why many empirical formulas have been developed. In Appendix I, empirical formulas for γ_{CJ} and γ as well as formulas for direct estimation of detonation pressure, explosion pressure and borehole pressure have been collected from literature.

1.2 Pressure measuring methods

If different pressures in a blast hole as illustrated in Fig. 1 are measured, we will have good information to determine the ideality of the detonation, matching of the explosive to the rock and partitioning of the explosive energy and to predict blasting results.

However, such measurements have not become a routine practice in rock blasting, owing to the technical difficulties and lack of feasible methods.

The manganin gage /7/ for measuring of detonation pressure is actually the only established method and commercial products are available. However, this method is mostly suitable in laboratory tests and the accessories are clumsy.

PVDF gages have also been employed in measuring detonation pressure with good success /8/. Since they are a type of piezo electrical gages with limited time constants, they are not suitable for measurement of the history of borehole pressure.

The composite carbon resistor has commonly been used as pressure sensor for detonation pressure since the first application by Watson /9/. This kind of gages can be applied in the measurement of not only strong shock pressures such as detonation pressures /9/, but also weak dynamic pressures such as pressure waves in rock masses /10, 11/ or static pressures.

Wilson et al. /12/ have used carbon resistor gages to measure the history of borehole pressure with good success. However, in their field application of the gage construction, the sensor is affected by the heat of the detonation gases after approximately 4 ms /12/.

Based on a sensor of a composite carbon resistor, G Persson at SveBeFo has developed another gage design named LHM /4/. The goal was to measure the entire history of the borehole pressure. Details are described in the following section.

1.3 The LHM method

The configuration of the LHM method /4/ is illustrated in Fig. 2. A sensor consisting of a carbon resistor (1/8 W, 470 Ω ± 5%) is mounted at the bottom of a steel cup. A signal cable connects the sensor through the bottom of the cup to an amplifier. The cup is filled with pure water. The size of the cup is 140 mm in length, 27 mm in inner diameter, 5 mm in side wall thickness and 20 mm in bottom thickness.

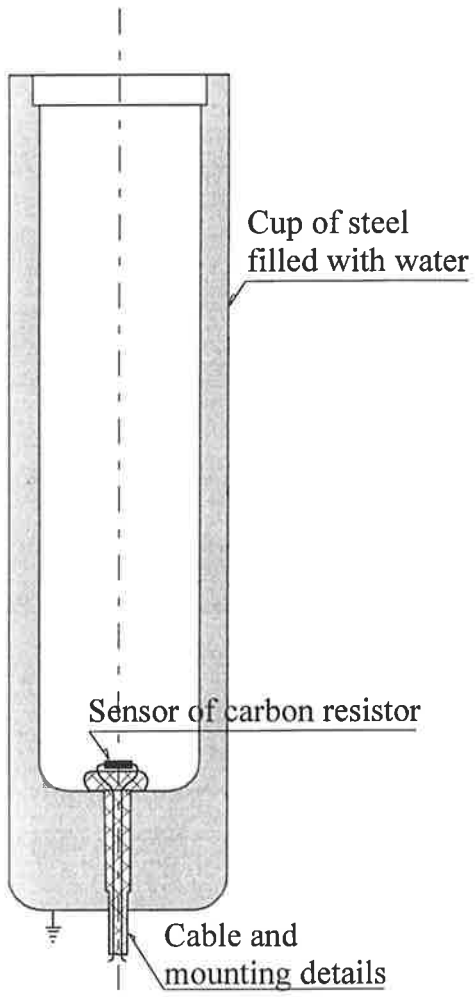

Fig. 2: The LHM gage design for measurement of history of borehole pressure.

The pressure sensitivity of the carbon resistor has been calibrated under static pressure up to 2.1 GPa /4/ and the pressure-resistance relation can be described by:

$$P = 0.4075\left(\frac{R_0 - R}{R}\right)^{0.8734} \quad \text{when } P \le 1 \text{ GPa} \tag{7a}$$

$$P = 0.2597\left(\frac{R_0 - R}{R}\right)^{1.3128} \quad \text{when } P \ge 1 \text{ GPa} \tag{7b}$$

where: P = pressure on the resistor (GPa)
R_0 = resistance of the carbon resistor at 1 atm (Ω), the nominal value is 470 Ω
R = resistance of the carbon resistor under pressure (Ω)

A comparison of this calibration result with calibrations carried out by other researchers is shown in Fig. 3.

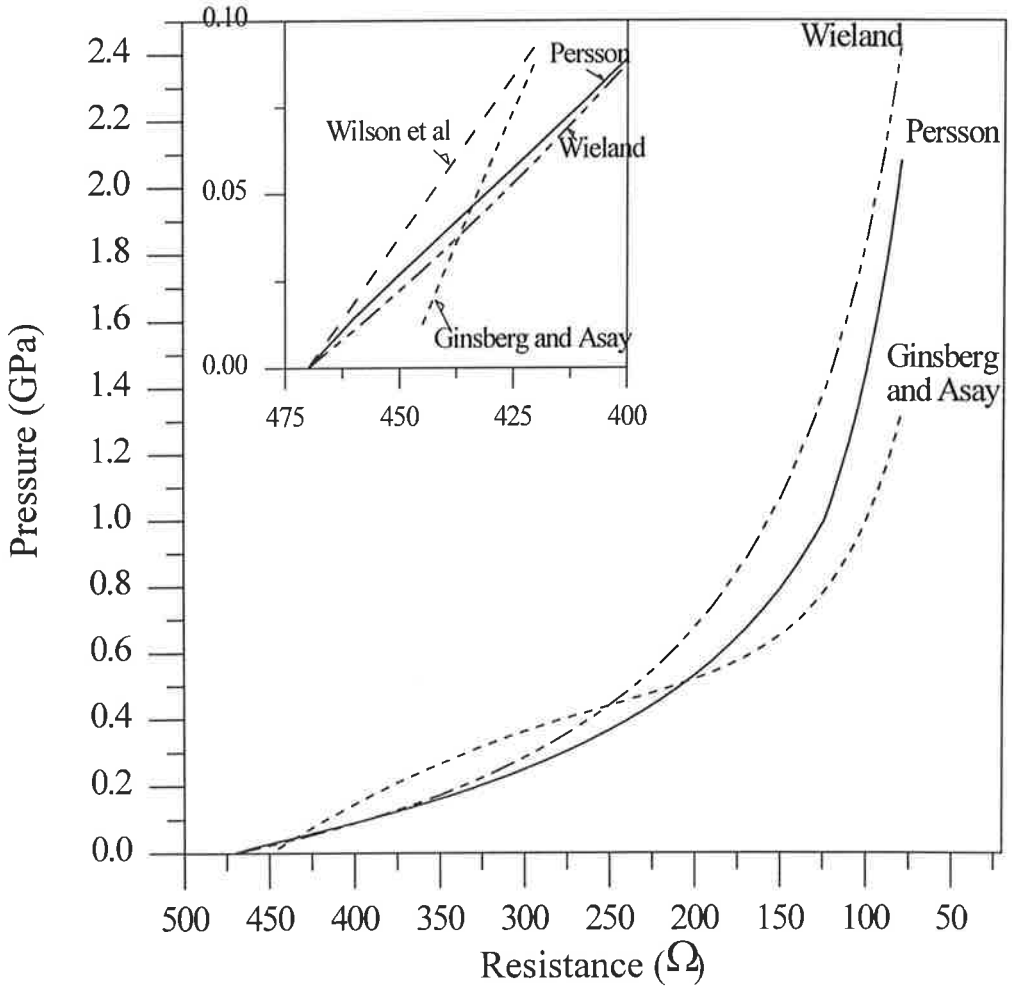

Fig. 3: Calibration of pressure sensitivity of the 1/8 W, 470 Ω carbon resistor carried out by Wilson et al /12/, Wieland /10/, Ginsberg and Asay /13/ and Persson /4/. Eqs. 7a and 7b originated from the calibration by Persson /4/.

When measuring, the cup is placed at the bottom of a blast hole with the water in contact with the explosive. The water protects the sensor from the high temperature detonation gases and also damps the strong shock wave. In this manner, the gage will only measure the pressure of a quasi-static state, corresponding to the borehole pressure. If the cup is fixed in the blast hole, it experiences the expansion of the blast hole and monitors the decrease of the borehole pressure during the expansion.

Laboratory tests with the LHM method have been carried out and very good results have been achieved /4/.

2 MEASUREMENTS IN BLAST HOLES IN GRANITE BLOCKS

2.1 Geometry of the experiments

Experiments have been carried out in seven blocks in Svenneby ornamental stone quarry. The rock there is a competent granite. The blocks used for the experiments were selected from big boulders without visible cracks or joints. The shape of the blocks was quite rectangular with flat surfaces and the size was 1.5 to 2.8 m in length, 1.0 to 1.4 m in width and around 1 m in thickness.

In six of the seven blocks, a blast hole and a cable hole were drilled in the middle part of each block parallel to the thickness dimension, see Fig. 4. The diameter of the blast hole was 38 mm and the length was approximately 0.6 m. A cable hole of 19 mm in diameter was drilled, coaxially with the blast hole, from the bottom of the blast hole to the opposite surface of the block. The length of the cable hole was therefore approximately 0.4 m. In the seventh block, only a blast hole of 38 mm in diameter and 730 mm in length was drilled.

2.2 Measuring system

The measuring system is shown in Fig. 5. In the six blocks where cable holes were drilled, an LHM pressure gage was placed at the bottom of each blast hole. The signal cable ran through this cable hole and connected the sensor to the amplifier. In the seventh block where no cable hole was drilled, the LHM gage was turned upside down and placed on top of the explosive. This test shot was aimed to verify whether the location of the LHM gage affects the measuring results. However, during the operation, the LHM gage was jammed in the hole and an air gap of approximately 80 mm was left between the gage and the explosive. Sand stemming was placed above the gage.

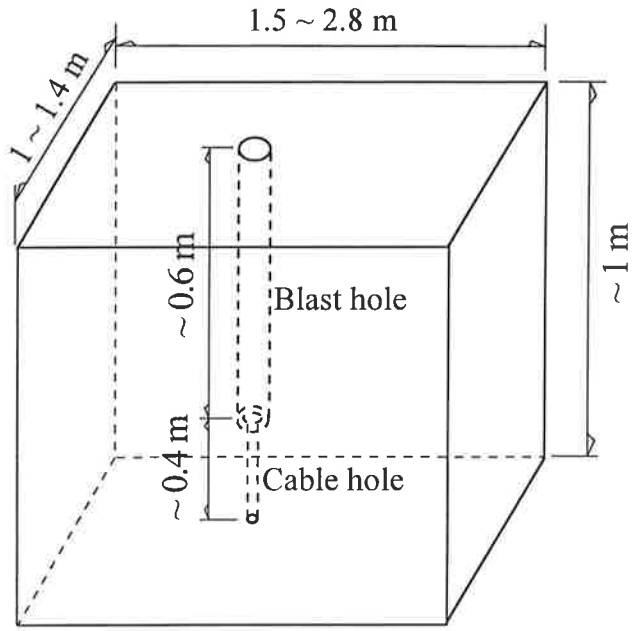

Fig. 4: Sizes of the six blocks and the drill holes where the borehole pressure measurements were carried out.

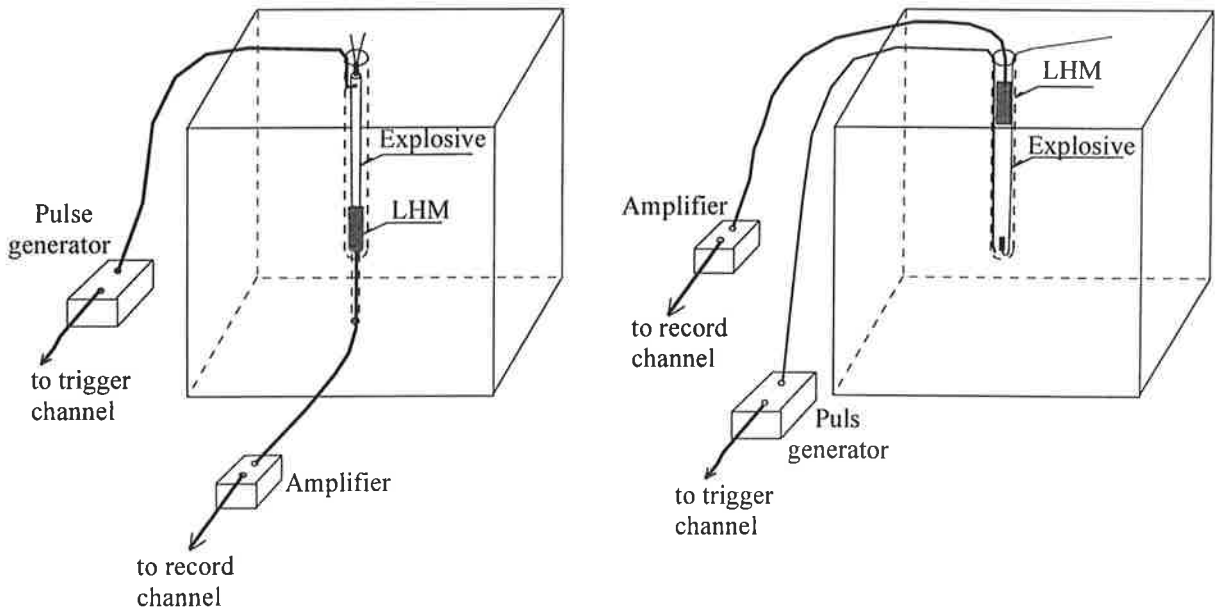

Fig. 5: Measuring system for borehole pressure measurements in granite blocks.
a): the arrangement in the six blocks with cable holes.
b): the arrangement in the seventh block without cable hole.

Top initiation was used in the six blocks with cable holes while bottom initiation was used in the seventh block, see Fig. 5. In either case, a pair of ionisation pins were placed in the explosive charge in the vicinity of the detonator. The ionisation signal was used for two purposes: to trig the recording equipment, a LeCroy 9354A digital oscilloscope, and to identify the initiation time of the explosive.

The reason for the top initiation in the six blocks is the usage of the fuse detonators in order to avoid any possible electric noise, see Section 3.4 for noise analysis. The diameter of the fuse is so large that it may affect the centring of the charge in the hole, if a bottom initiation would be used.

The function of the amplifier is to convert the resistance change in the carbon resistor into a voltage change and output this voltage change to the oscilloscope. To avoid reflections in the cable, a 50 ohm impedance match has been employed from the amplifier to the oscilloscope.

2.3 Tested explosives and charging method

Two explosives were studied. One is Gurit B and the other is the so-called "Blue Cartridge" (Blå rör in Swedish). Both are designed for cautious blasting and are cap sensitive. The properties of these two explosives are listed in Table 1 below. The nominal values are provided by the manufacturer Dyno Nobel AB, and the measured values came from our tests.

Table 1: Properties of the two tested explosives

Explosive	Density in cartridge (kg/m^3)		VOD in ϕ 16 mm charge (m/s)		At ideal detonation*	
	Nominal	Measured	Nominal	Measured	Heat of detonation (MJ/kg)	VOD (m/s)
Gurit B	1000	1050	2000	2065	3.51	5945
Blue Cartridge	1000	1000	1650	1946	1.94	4221

*: Calculated by program Cheetah /14/

Besides, a series measurements of unconfined VOD (velocity of detonation) and charge density have been carried out on Gurit B, in which the charge diameter has been varied from 16 mm to 49.2 mm, see details in Appendix II. Based on the measurements, the relation between the VOD and the inverse charge diameter can be expressed by:

$$VOD = 3857 - 28674/d \qquad (8)$$

where: VOD = VOD of unconfined Gurit B at the density of 1050 kg/m^3 (m/s)
d = charge diameter of Gurit B (mm)

Seven test shots were fired. Only one No. 8 detonator was used for the initiation of each shot. The explosive studied in each test shot and the charging method are summarized in Table 2.

Table 2: The explosive used and the charging method in this study

Test No.	Explosive studied	Charge length (m)	Diameter (mm)		Decoup-ling ratio	Charge density (kg/m^3)	Charging method
			Hole	Charge			
1	Blue Cartridge	0.50	38	16	2.375	1000	ϕ 17 mm cartridge
2	Blue Cartridge	0.50	38	16	2.375	1000	ϕ 17 mm cartridge
3	Gurit B	0.51	38	21.2	1.792	1050	ϕ 22.5 mm cartridge
4	Gurit B	0.61	38	21.2	1.792	1050	ϕ 22.5 mm cartridge
5	Gurit B	0.43	38	38	1	980	fully charged *
6	Gurit B	0.47	38	38	1	1070	fully charged *
7**	Gurit B	0.33	38	38	1	960	fully charged *

*: The explosive was taken from ϕ 22.5 mm cartridges, weighed and carefully charged in the blast hole to ensure an even charge density in the blast hole.

**: Test No. 7 differs from the other tests, as it was carried out in the block without a cable hole, see Fig. 5b.

3 MEASURING RESULTS AND ANALYSIS

The pressure measurements and VOD estimates from the seven shots are summarized in Table 3, together with the charge configuration. Pressure signals are shown in Figs. 6 and 7. The signals are also shown in details in Appendix IV. Furthermore, in Appendix IV, the photos of the LHM gages recovered after the blasting experiments are also shown.

Table 3: Results of borehole pressure measurements in seven granite blocks

Test No.	Explosive	Charge		Hole diameter (mm)	Pressure measured		Estimated VOD in hole* (m/s)
		Diameter (mm)	Density (kg/m^3)		Max. (GPa)	Duration (μs)	
1	Blue Cartridge	16	1000	38	0.08	500	1900
2	Blue Cartridge	16	1000	38	0.12	420	2300
3	Gurit B	21.2	1050	38	> 0.60	30	2460
4	Gurit B	21.2	1050	38	0.81	300	2640
5	Gurit B	38	980	38	1.38	86	3090
6	Gurit B	38	1070	38	1.30	100	3470
7**	Gurit B	38	960	38	1.70	36	—

*: Estimated VOD = VODs in blast holes estimated from the pressure signals, see explanation in Section 3.1.

**: Test No. 7 differs from the other tests as it was carried out in the block without cable hole, see Fig. 5b.

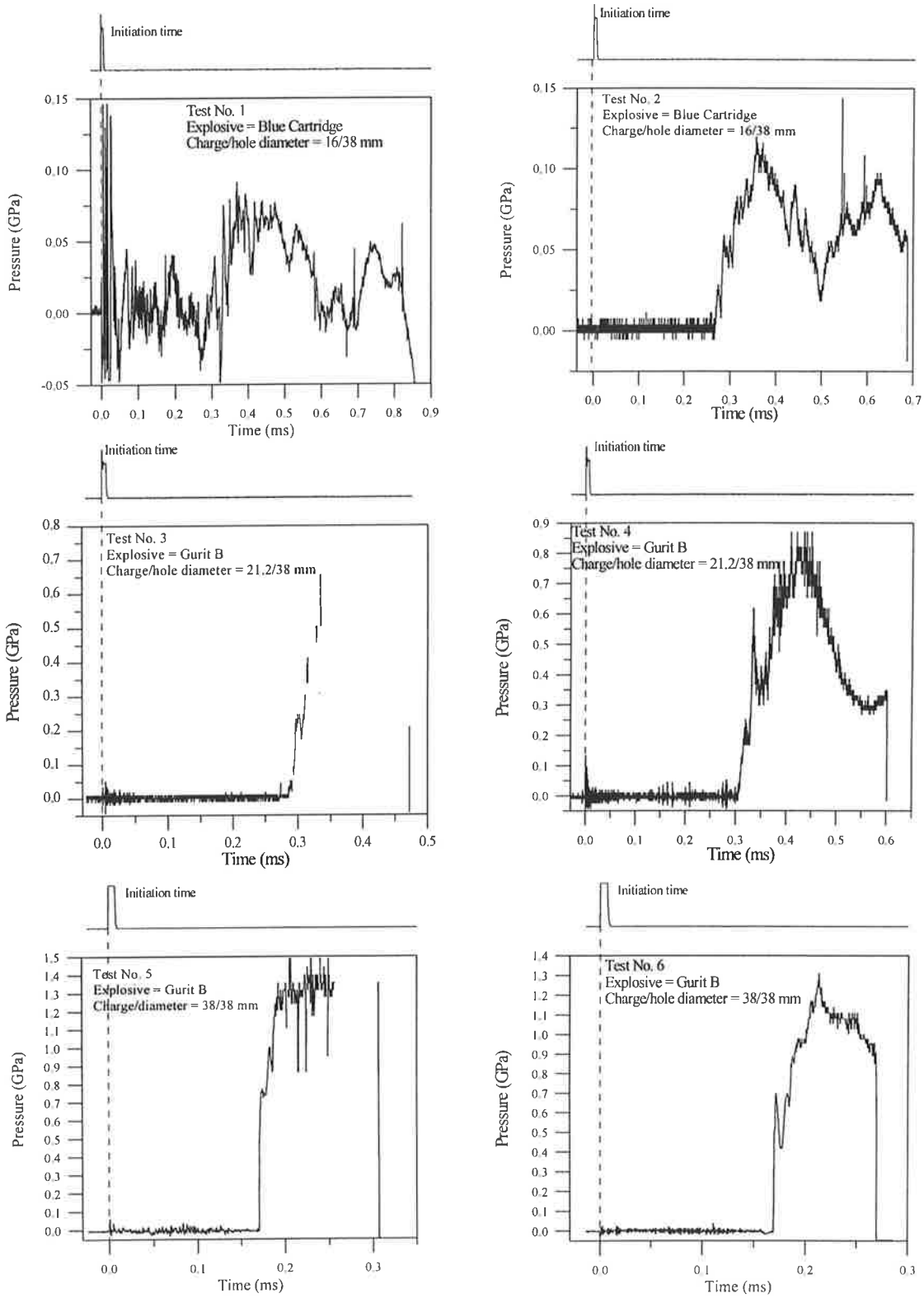

Fig. 6: Pressure signals from the six LHM gages mounted in the bottom of the blast holes in granite blocks, corresponding to test No. 1 to 6 in Tables 2 and 3.

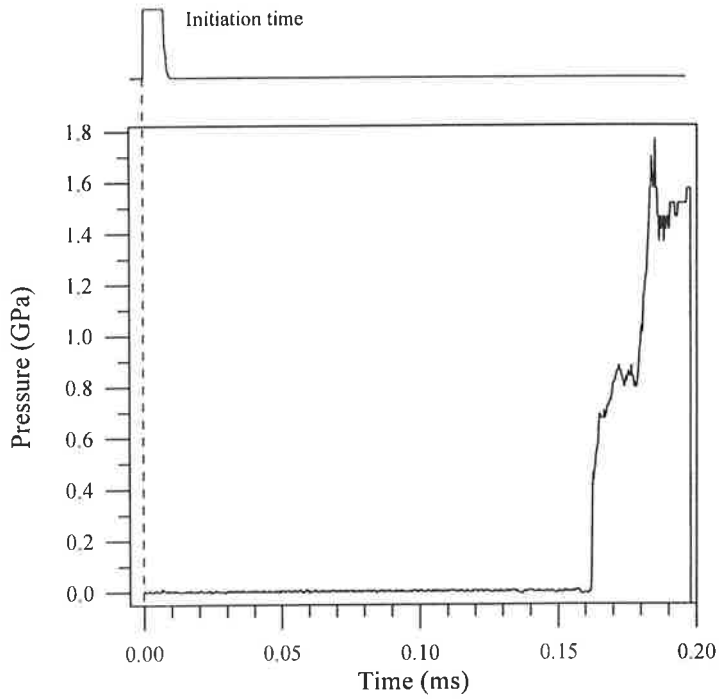

Fig. 7: Pressure signal from the seventh LHM gage mounted on top of the explosive, corresponding to test No. 7 in Tables 2 and 3.

3.1 Velocity of detonation in blast hole

Since the explosive was initiated at the top, no direct VOD measurements could be carried out in the blast holes. Thus, the VODs in the explosives were estimated based on the pressure signals and the ionisation signals from the ionisation pins.

The ionisation signal indicates the initiation of the explosive. The pressure arrival at the pressure sensor can be read from the pressure signal. The time between these two instants is the sum of the detonation duration in the explosive and the shock propagation time in the water column in the LHM cup. Since the lengths of the explosive charge and the water column were known, the VOD can be estimated, provided that the shock propagation time in the water column in the LHM cup is known. The estimation procedure is described in the following and the results are shown in Table 4.

Firstly, the shock wave velocity in the water in the LHM cup is estimated.

Notice that there is a distance between the pressure sensor and the bottom of the LHM cup, see Fig. 2. The incident shock wave in the water first arrives at and impacts the sensor, then it will continue to propagate until the bottom of the LHM cup. There, the shock wave will be reflected and the reflected wave will propagate back towards the

pressure sensor. When the reflected wave reaches the sensor, it will collide with the incident wave there.

Table 4: Estimation of the VODs in the explosives in the blast holes.

Test No.	Type of explosive	Charge		Hole diameter	Estimated velocity		Reference VOD	
		Diameter (mm)	Density (kg/m^3)	(mm)	Shock wave in water[1] (m/s)	VOD in hole[2] (m/s)	Uncon-fined[3] (m/s)	Ideal[4] (m/s)
1	Blue Cartridge	16	1000	38	1250	1900	1946	4221
2	Blue Cartridge	16	1000	38	1350	2300	1946	4221
3	Gurit B	21.2	1050	38	1560	2460	2504	5945
4	Gurit B	21.2	1050	38	1350	2640	2504	5945
5	Gurit B	38	980	38	2980	3090[5]	3103	5648
6	Gurit B	38	1070	38	2840	3470	3103	6020

[1]: Estimated from the pressure signals, see explanations in the text.

[2]: VODs in blast holes estimated from the pressure signals, see explanations in the text.

[3]: VODs measured in unconfined cartridges at the densities of 1000 kg/m^3 for Blue Cartridge and 1050 kg/m^3 for Gurit B, see Appendix II.

[4]: Calculated by program Cheetah /14/.

[5]: Note that the charge density in the hole is slightly lower than that in the unconfined cartridge.

In the pressure record, the first arrival of the incident shock wave at the sensor results in a sharp pressure rise. The collision of the reflected wave with the incident wave at the sensor results in a second rapid rise of pressure, see Fig. 8. Therefore, the time between the arrival of the incident wave and the arrival of the reflected wave at the sensor can be determined. During this time, the propagation distance of the shock wave is twice the gap widths between the sensor and the LHM bottom. The gap width was kept at 12.5 mm and the distance from the water surface to the sensor at 115 mm in all the LHM gages.

Knowing the distance and time, the shock wave velocity in the water was calculated.

After this, the propagation time of the shock wave in the water before it arrives at the sensor was calculated, based on the estimated shock wave velocity in the water and the known depth of water in the LHM cup.

Finally, the VOD in the explosive in the hole is estimated accordingly:

VOD = charge length/detonation duration

Detonation duration = pressure arrival time at the sensor (see Fig. 8) - initiation time of the explosive (see Fig. 8) - pressure propagation time in the water.

Pressure propagation time in the water = length of the water column in the LHM cup/velocity of the shock wave in the water.

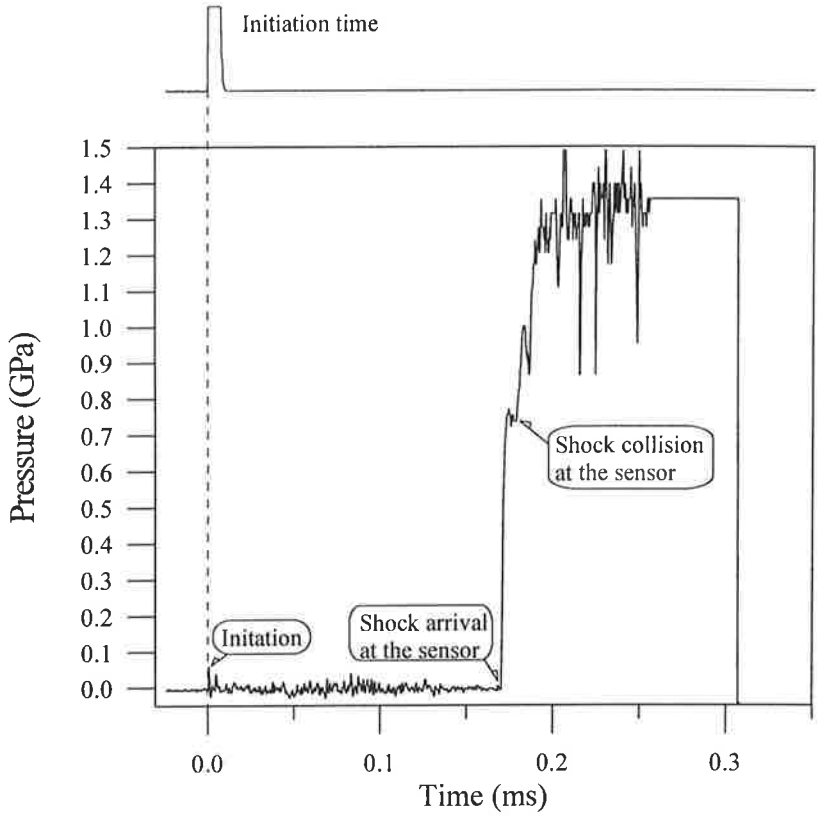

Fig. 8: Estimation of the shock wave velocity in the water in the LHM cup.

It should be noted that the above VOD estimates are subjected to a number of uncertainties. For example, the speed of the incident shock wave in water differs from that of the reflected shock wave. The length of the explosive charge may not be accurate since the detonator is inserted a certain distance inside the charge. Nevertheless, since the VODs could not be measured, the above estimation was considered to be the best we could do to the measurements. Also, judged from the measured VODs in unconfined charges, the estimated VODs seem reasonable.

3.2 Amplitude of the borehole pressure

3.2.1 Comparison of the measured borehole pressures with empirical estimates

The measured peak borehole pressure ranges from 0.08 to 1.7 GPa depending on the explosive type and the decoupling ratio. In this section the measured borehole pressures

are compared with the estimates from the empirical formulas collected in Appendix I. A thermodynamic program Cheetah with BKWR equation of state /14/ has also been used to calculate the different pressures of the studied explosives in the ideal detonation state.

The input parameter properties for the Cheetah calculation and for the empirical formulas may be found in Tables 1, 2, 3 and 4. However, the chemical formulas for the studied explosives are the properties of the manufacturer, Dyno Nobel AB, and hence can not be disclosed.

3.2.1.1 Estimation of the detonation pressure

Tables 5a and 5b show the estimates of the detonation pressure in the explosives for the six test shots. Actually, the γ_{CJ} value has been estimated for each test and then the detonation pressure was calculated by Eq. 1. It can be seen that all six empirical formulas estimated a γ_{CJ} of less than or roughly equal to 3 (Eq. A11). The variation of the estimated detonation pressures lies within ±12% of the average, which is very small. The variation could have been less, within ±7%, if Eq. A11 had been excluded. As expected, Cheetah gives higher detonation pressures than all other formulas, since it calculates ideal detonations and consequently gives higher detonation velocities and higher detonation pressures.

3.2.1.2 Estimation of the explosion pressure

Table 6 shows the estimates of the constant volume explosion pressure in the studied explosives by five formulas. The variation of the estimated explosion pressures lies within ±17% of the average, which is larger than that for the detonation pressure. Again, Cheetah gives higher explosion pressures than other formulas, as explained above.

In Test No. 5 and No. 6, the blast holes were fully charged. Thus the borehole pressure should be the same as the explosion pressure. Comparing the measured borehole pressures with the average estimate of the explosion pressure, the agreement for Test No.5 is good while rather poor for Test No. 6.

3.2.1.3 Estimation of the borehole pressure in decoupled blast holes

The borehole pressure in the four decoupled holes was estimated by two empirical formulas: Calder's formula /15/ (Eq. 9) and Atlas Powder formula /17/ (Eq. 10). These two formulas are actually the same as Eq. 6, substituting γ with a value of 1.2 and 1.3. In Table 7, the estimates were compared with the measured pressures in Tests No. 1 to 4.

Table 5a: Detonation pressures for Tests No. 1 to 6 estimated by empirical formulas in Appendix I. Parameter values for the formulas can be found in Tables 1, 3 and 4.

Eq.	Estimated γ_{CJ} and calculated P_{CJ}, GPa, by: $P_{CJ} = \rho_0 D^2/(1+\gamma_{CJ})$											
	Test 1		Test 2		Test 3		Test 4		Test 5		Test 6	
	γ_{CJ}	P_{CJ}	γ_{CJ}	P_{CJ}	γ_{CJ}	P_{CJ}	γ_{CJ}	P_{CJ}	γ_{CJ}	P_{CJ}	γ_{CJ}	P_{CJ}
A4	—	—	—	—	—	—	—	—	—	—	—	—
A6	—	—	—	—	2.49	1.82	2.49	2.10	—	—	2.49	3.69
A7	—	—	—	—	2.53	1.80	2.53	2.07	2.49	2.68	2.54	3.64
A8[1)]	2.37	1.07	2.37	1.57	2.46	1.84	2.46	2.12	2.36	2.79	2.48	3.70
A9	—	—	—	—	2.18	2.00	2.18	2.30	2.14	2.98	2.20	4.03
A11	≈ 3	≈0.90	≈ 3	≈1.32	≈ 3	≈1.59	≈ 3	≈1.83	—	—	≈ 3	≈3.22
A12	2.48	1.04	2.48	1.52	2.50	1.82	2.50	2.09	2.47	2.70	2.50	3.68
Che-etah[2)]	3.70	3.80	3.70	3.80	2.84	9.66	2.84	9.66	2.77	8.39	2.86	10.04

—: condition(s) for the empirical formula not satisfied: either the density or the chemical formula of the explosive is beyond the application conditions.

[1)]: the heat of detonation and the ideal VOD in Eq. A8 were calculated by Cheetah /14/, see Table 1.

[2)]: thermodynamic program Cheetah /14/.

Table 5b: Summary of empirical estimates of detonation pressure for the six test shots.

	Test 1	Test 2	Test 3	Test 4	Test 5	Test 6
Average estimate of P_{CJ}*	1.00	1.47	1.81	2.09	2.79	3.66
Deviation of the estimates from the average	-10% ~ +7%	-10% ~ +7%	-12% ~ +10%	-12% ~ +10%	-4% ~ +7%	-12% ~ +10%

*: The average estimate does not include the calculated values by program Cheetah /14/.

$$P_b = P_e \cdot \left(\sqrt{\frac{L_e}{L_b}} \cdot \frac{r_e}{r_b} \right)^{2.4} \qquad (9)$$

Where: $P_e = N(\rho_0)\, \rho_0\, D^2$

$N(\rho_0)$ = a constant varying with ρ_0 /15/

$= 0.235\rho_0^{-0.57} - 0.08$, when $800 \le \rho_0 \le 2000$ /16/

ρ_0 = density of the explosive (kg/m^3)

D = VOD (m/s)

P_e, L_e, L_b, r_e, r_b = see Eq. 6

Table 6: Estimated explosion pressures for Tests No. 1 to 6 by empirical formulas in Appendix I and measured explosion pressures from Tests No. 5 and 6. Parameter values for the formulas can be found in Tables 3 and 5.

Eq.	Ref.	Estimated explosion pressure: P_e (GPa)					
		Test 1	Test 2	Test 3	Test 4	Test 5	Test 6
A13*	/6/	0.50	0.74	0.91	1.04	1.39	1.83
A14	/15/	0.56	0.82	0.94	1.09	1.45	1.88
A15	/A12/	0.41	0.60	0.72	0.82	1.05	1.45
A16	/A13/	0.46	0.67	0.79	0.91	1.20	1.58
A17	/16/	0.47	0.68	0.79	0.91	1.22	1.77
Average		0.48	0.70	0.83	0.95	1.26	1.70
Deviation from the average		-15% ~ +17%	-15% ~ +17%	-13% ~ +13%	-14% ~ +15%	-17% ~ +15%	-15% ~ +11%
Measured explosion pressure						**1.38**	**1.30**
Errors between estimates and measurement						-24% ~ +5%	+11% ~ +45%
Cheetah	/14/	1.62	1.62	4.46	4.46	3.89	4.63

*: The value of P_{CJ} in Eq. A13, $P_e = P_{CJ}/2$, was taken as the average estimate of P_{CJ} in Table 5b.

Table 7: Measured borehole pressures in decoupled blast holes from Tests No. 1 to 4 and estimates from Eq. 6 with two empirical γ values.

		Borehole pressure in decoupled holes: P_b (GPa)				Eq.	Ref.
		Test 1	Test 2	Test 3	Test 4		
Measured		**0.08**	**0.12**	**> 0.6**	**0.81**	—	—
Calder formula	Estimate	0.070	0.10	0.23	0.27	9	/15/
	Error	-13%	-17%	>-62%	-67%	—	—
Atlas Powder formula	Estimate	0.05	0.07	0.17	0.20	10	/A13/
	Error	-38%	-42%	>-73%	-75%	—	—
Cheetah	isentrope*	0.04	0.04	0.30	0.30	—	/14/
	explosion*	0.06	0.06	0.58	0.58	—	/14/

*: For each test shot in Table 7, there are two borehole pressures obtained from two types of Cheetah calculations. In the first Cheetah calculation, "Cheetah isentrope", the constant volume explosion state of the explosive was calculated first. Then, the explosion gases were isentropically expanded to fill the borehole. At this stage, the pressure in the detonation gases was taken as the borehole pressure. In the second calculation, "Cheetah explosion", the unreacted explosive was first uniformly distributed in the whole borehole. Then the constant volume explosion state in the diffused explosive was calculated and taken as the borehole pressure.

$$P_b = P_e \cdot \left(\sqrt{\frac{L_e}{L_b}} \cdot \frac{r_e}{r_b} \right)^{2.6} \qquad (10)$$

Where: $P_e = \rho_0 D^2/8$

ρ_0, D = see Eq. 9

P_e, L_e, L_b, r_e, r_b = see Eq. 6

Generally speaking, the agreement between the empirical estimates of the borehole pressure and the measurements is poor. The worst agreement is obtained for decoupled charges with a small decoupling ratio, i.e. Tests No. 3 and No. 4. Calder's formula estimates quite well the borehole pressure in holes with large decoupling, i.e. Tests No. 1 and No. 2.

The six measurements of borehole pressure and the scatter of the corresponding estimtes are illustrated in Fig. 9.

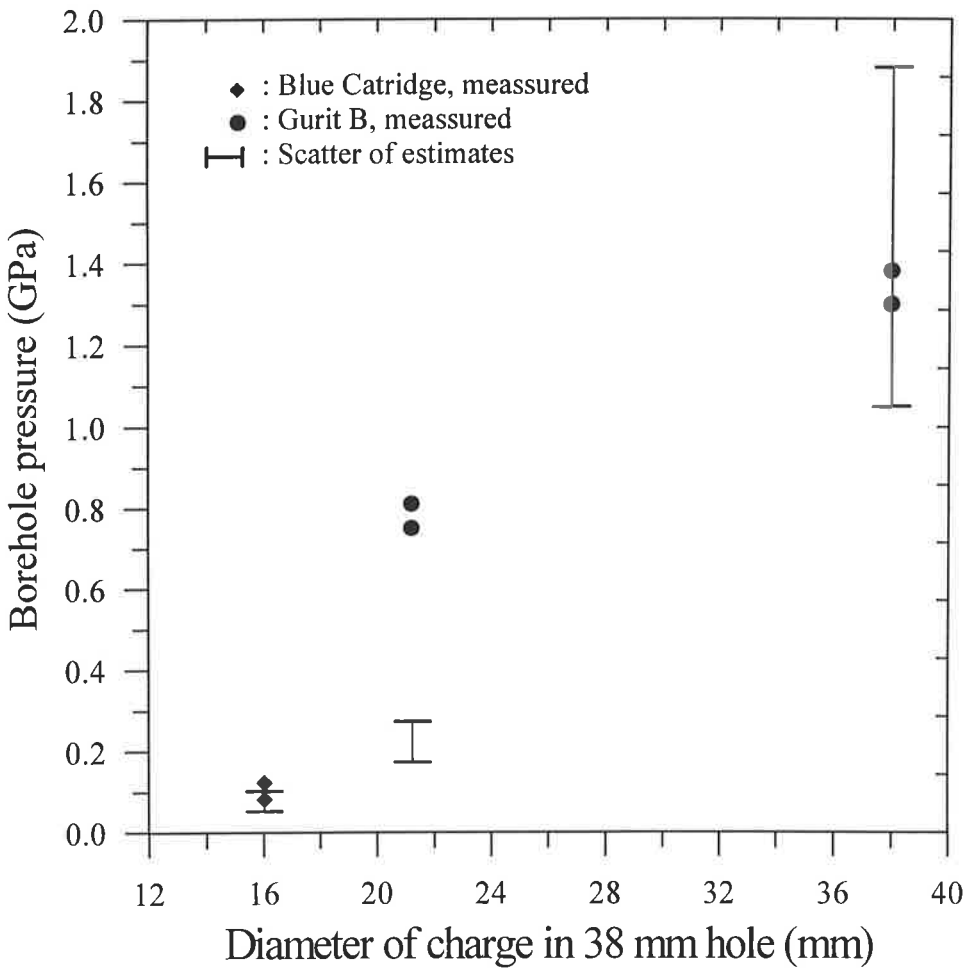

Fig. 9: Comparison between the measured and the estimated borehole pressures.

3.2.1.4 Conclusions for the estimations

From the analyses in Sections 3.2.1.1 to 3.2.1.3, the following conclusions can be drawn for the pressure estimations of the test explosives:

- Detonation pressure: Different empirical formulas give similar predictions. The variation of the predictions is within ±12%. However, there are no measurements to calibrate the predictions.

- Explosion pressure: The variations between different predictions are within ±17%. Compared the estimates with two measurements, the agreement is rather good. Based on Test No. 5, the best agreement is achieved by Eq. A13 or Eq. 2 combined by Eq. A8, i.e.

$$P_e = \tfrac{1}{2}\cdot P_{CJ} = \tfrac{1}{2}\cdot\rho_0 D^2/(\gamma_{CJ}+1) \text{ and } \gamma_{CJ} = \sqrt{1+\frac{D_\infty^2}{2(q+e_0)}}$$

- Borehole pressure in decoupled hole: At a large decoupling (decoupling ratio 2.375), estimates given by Calder's formula agree well with the measurements. However, at a smaller decoupling, the agreement between the predictions by the empirical formulas and the measurements is very poor. The error is as large as 75%.

3.2.2 Analysis of discrepancies between the measured and estimated borehole pressure

The discrepancies are analyzed in two respects, the accuracy of the measurements and the principle behind the estimations.

Since the number of the measurements is limited, it is difficult to statistically obtain an accuracy of the measurements. The largest uncertainty lies in the VOD values, since no direct VOD measurement has been carried out and the VOD values have been estimated from the pressure signals. However, judged from the measured VODs in unconfined charges, the estimated VODs seem reasonable, see Table 4.

3.2.2.1 Analysis of the explosion pressure

Generally speaking, the borehole pressure increases as the product of explosive density and squared VOD increases ($\rho_0 \cdot D^2$). This general dependence is obeyed in the pressure measurements from Tests No. 1 to 4, but not in Tests No. 5 and No. 6. Both the charge density and the VOD are higher in Test No. 6 than in Test No. 5, while the measured pressure is higher in Test No. 5. This might be an inaccuracy of the pressure measurement, which consequently results in a large discrepancy between the estimated

and measured explosion pressures for Test No. 6, see Table 6. Otherwise, the agreement is good between the measured and the estimated explosion pressures, see Table 6.

3.2.2.2 Analysis of the borehole pressure in decoupled holes

There are four measurements, Tests No. 1 to 4. The measurements showed that the borehole pressure increases as the VOD increases. Tests No. 3 and 4 showed also that the pressure in decoupled boreholes is lower than that in fully charged holes.

However, compared to the measurements, the empirical formulas did not give good estimates of the borehole pressure in decoupled holes. In fact, the discrepancies are large, especially for the cases of small decoupling, as described in Section 3.2.1.4. The reason for the discrepancy might originate in the calculation principle behind the formulas.

As described in Section 1.1, Eqs. 3 to 6, the empirical formulas calculate the pressure inside the detonation gases when the gases have isentropically expanded to fill the borehole. In other words, the borehole pressure is a point on the gas expansion isentrope corresponding to the volume of the blast hole. However, there are two defects in such an estimation, a) the actual gas expansion in blast holes is not an isentropical process and b) the adiabatic gamma (γ) in the formulas is not a constant during the expansion. Therefore, Eqs. 4 to 6 are not mathematically correct.

Look at the blasting in a decoupled borehole. First, the detonation gases shock the air in the gap between the explosive and the borehole wall. This results a rarefaction wave back into the detonation gases and a shock wave into the air. When this air shock wave arrives at the borehole wall, a new shock wave will be reflected into the air and further into the detonation gases. Due to the cylindrical symmetry, this shock - reflection process will continue long after the borehole wall starts to move.

Nevertheless, if the decoupling is sufficiently large, the reflection from the borehole wall is weak and less significant. The expansion process may be estimated by a pure isentrope. Furthermore, when the decoupling is large and consequently the gas expansion is large before the reflection, the adiabatic gamma of the detonation gases (γ) may be considered as a constant around 1.2 to 1.3. This can partially explain why the Calder's formula (Eq. 9) gives good estimate at large decoupling, see Table 7 and Section 3.2.1.4.

3.2.3 A new estimation formula for borehole pressure in decoupled holes

3.2.3.1 Estimation principle: concept of the "Spread Charge"

Based on the discussion above, a new estimation principle will be presented.

In a decoupled blast hole, the explosive is normally concentrated in the central part of the hole. The explosive charge in this manner is hereinafter referred to the "concentrated charge". If, instead, the explosive is spread into the whole blast hole, there will not be any decoupling. In other words, the blast hole is fully charged with a new "charge" which has exactly the same chemical composition as the original "concentrated charge", yet its density is lower so that it fully fills the blast hole. Define this new charge as the "Spread Charge". Then, the borehole pressure in a decoupled hole with a "concentrated charge" becomes the explosion pressure in the corresponding "Spread Charge". In this way, the expansion isentrope is not involved in the calculation.

If the VOD of the "Spread Charge" could be estimated, the explosion pressure would be easily estimated by any of the empirical formulas mentioned in Section 3.2.1.2, i.e. Eqs. A13 to A17 in Appendix I. However, to estimate or to measure the VOD in such a charge is not a simple operation. If the decoupling is large, the density of the "Spread Charge" is very low. It may not be detonable at all in reality.

Another method is to consider the detonation Hugoniot of the "Spread Charge", as described in the following section and illustrated in Fig. 10.

3.2.3.2 Estimation formula

Based on the concept of "Spread Charge", the borehole pressure in a decoupled hole can be calculated.

The detonation Hugoniot for any explosive is the combination of the energy conservation in the detonation (Eq. 11) and the energy equation of that explosive (Eq. 12).

$$e_1 - e_0 = q + \tfrac{1}{2}(P_1 + P_0)(v_0 - v_1) \quad (11)$$

$$e = e(P, v) \quad (12)$$

where: e_1, P_1, v_1 = state variables in the reacting explosive: specific internal energy (J/kg), pressure (Pa) and specific volume (m^3/kg) respectively

e_0, P_0, v_0 = state variables in the unreacted explosive: specific internal energy (J/kg), pressure (Pa) and specific volume (m^3/kg) respectively

q = specific chemical energy converted to mechanical energy in detonation (J/kg)

e = the internal energy of the explosive at any state (P, v).

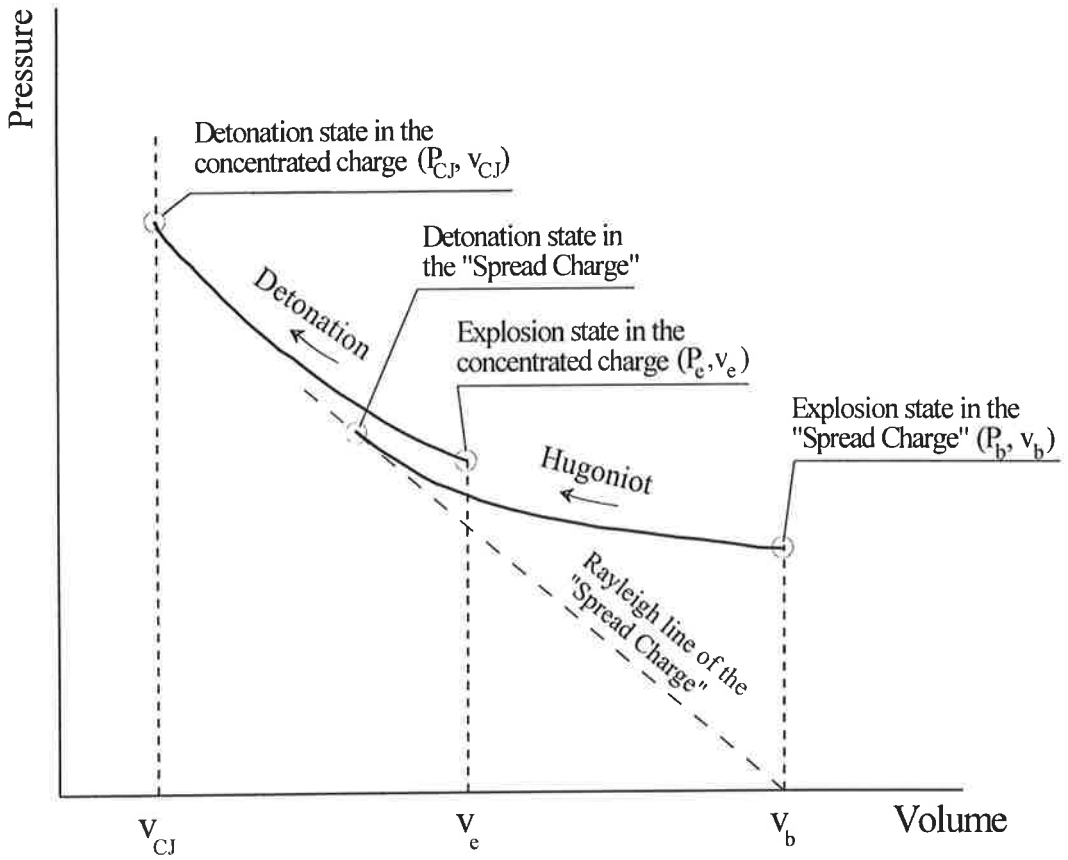

Fig. 10: Principle of estimating borehole pressure in a decoupled blast hole as a state on the detonation Hugoniot of the "Spread Charge". In the figure, v_{CJ} = specific volume of the "concentrated charge" at CJ state, v_e = specific volume of the "concentrated charge" at the ambient state and v_b = volume of the borehole per kg explosive = specific volume of the "Spread Charge" at the ambient state. The detonation Hugoniot of the "concentrated charge" goes from (P_e, v_e) to (P_{CJ}, v_{CJ}), while the detonation Hugoniot for the "Spread Charge" goes from (P_b, v_b) to the detonation state of the "Spread Charge".

If the specific internal energy of the reacting explosive obeys the γ-law EOS, i.e.

$$e = e(P,v) = \frac{Pv}{\gamma - 1} \tag{13}$$

where: e, P, v = state variables on the detonation Hugoniot, specific internal energy (J/kg), pressure (Pa) and specific volume (m^3/kg) respectively
γ = adiabatic gamma. Note that it is not necessarily a constant

Applying the γ-law EOS on a specific state (P_1, v_1) on the detonation Hugoniot:

$$e_1 = \frac{P_1 v_1}{\gamma_1 - 1} \tag{14}$$

where: e_1, P_1, v_1 = state variables at a specific state on the detonation Hugoniot, specific internal energy (J/kg), pressure (Pa) and specific volume (m^3/kg) respectively

γ_1 = adiabatic gamma at the specific state on the detonation Hugoniot

then, the detonation Hugoniot can be reduced from the conservation of energy in a detonation (Eq. 11) by replacing specific energy, e_1, by Eq. 14:

$$P_1 = \frac{2(q + e_0) + P_0(v_0 - v_1)}{\frac{\gamma_1 + 1}{\gamma_1 - 1} v_1 - v_0} \tag{15}$$

For any explosive, the pressure at the constant volume explosion is the pressure on the detonation Hugoniot at $v_1 = v_0$ and can be calculated by substituting v_1 by v_0 in Eq. 15:

$$P_{explosion} = (\gamma_{explosion}-1)(q+e_0)/v_0 \tag{16}$$

where: $P_{explosion}$ = constant volume explosion pressure (Pa)

$\gamma_{explosion}$ = adiabatic gamma at the explosion state

q, e_0, v_0 = see Eq. 11

Before applying Eq. 16 on the "concentrated charge" respectively the "Spread Charge", consider the internal energy of these two charges.

For solid explosives, the specific internal energy of the unreacted explosive, e_0, is usually negligible. Thus, e_0 can be set to zero for both charges. Furthermore, since the "Spread Charge" has exactly the same chemical composition as the original "concentrated charge", the specific detonation energy, q, should be the same for both the explosives.

Therefore, $q+e_0$ is the same for both the "concentrated charge" and the "Spread Charge". Besides this, other necessary parameters are:

For the "concentrated charge":

$P_{explosion} = P_e$ = explosion pressure of the "concentrated charge" (Pa)

$\gamma_{explosion} = \gamma_e$ = adiabatic gamma of the "concentrated charge" at the explosion state

$v_0 = v_e$ = specific volume of the "concentrated charge" at the ambient state (m^3/kg)

For the "Spread Charge":

$P_{explosion} = P_b$ = explosion pressure of the "Spread Charge"
= borehole pressure in the decoupled hole charged with the corresponding "concentrated charge" (Pa)

$\gamma_{explosion} = \gamma_b$ = adiabatic gamma of the "Spread Charge" at the explosion state

$v_0 = v_b$ = specific volume of the "Spread Charge" at the ambient state (m^3/kg)
= the borehole volume per kg explosive (m^3/kg)

Now, applying Eq. 16 to the "concentrated charge" respectively the "Spread Charge", a relation between the borehole pressure in a decoupled hole, P_b, and the explosion pressure of the "concentrated charge" in the hole, P_e, can be established.

$$P_e = (\gamma_e - 1)(q + e_0)/v_e \quad (17)$$

$$P_b = (\gamma_b - 1)(q + e_0)/v_b \quad (18)$$

$$P_b = \left(\frac{\gamma_b - 1}{\gamma_e - 1}\right) \cdot \left(\frac{v_e}{v_b}\right) \cdot P_e \quad (19)$$

where: P_e = explosion pressure of the "concentrated charge" (Pa)
P_b = explosion pressure of the "Spread Charge" (Pa)
= borehole pressure in a decoupled hole with the "concentrated charge" (Pa)
v_e = volume of the "concentrated charge" at the ambient state (m^3)
v_b = volume of the borehole (m^3)
γ_e = adiabatic gamma of the "concentrated charge" at its explosion state
γ_b = adiabatic gamma of the "Spread charge" at its explosion state
q, e_0 = heat of detonation (J/kg) and specific internal energy before detonation for both charges

Again, the difficulty is how to obtain suitable values for the γ_e and γ_b. Therefore, as an engineering solution, one more assumption is introduced. i.e. $\gamma_e = \gamma_b$. By doing so, Eq. 19 is simplified into:

$$P_b = (v_e/v_b) \cdot P_e \quad (20)$$

or:

$$P_b = P_e \cdot \left(\sqrt{\frac{L_e}{L_b}} \cdot \frac{r_e}{r_b}\right)^2 \quad (21)$$

Here: P_e = explosion pressure in the explosive (Pa)
P_b = borehole pressure in the decoupled blast hole (Pa)
L_e = length of the charge (m)
L_b = length of the borehole (m)
r_e = radius of the charge (m)
r_b = radius of the borehole (m)

Eq. 21 is simple and suitable for engineering purposes. However, it complied with two assumptions, i.e., a) the specific energy of the reacted explosive obeys the γ-law EOS and b) the γ value is the same at v_0 and at v_b. In the case that complexity is allowed, a more realistic form of EOS such as JWL EOS may be used to describe the specific energy of the reacted explosive. Then, the calculation can even be done independent of the above-mentioned assumptions.

An even more complicated and accurate estimation method is to construct a burning model for the explosive and simulate the dynamic process using a computer code, see example in /18/.

3.2.3.3 Estimated borehole pressures for the test shots using the new formula

Eq. 21 was used to estimate the borehole pressures in the four test shots with decoupled charges. Estimates were shown in Table 8. The estimation error for decoupled holes with large decoupling ratio is still large, around -60%. The reasons to this large error could be the accuracy in the measurements, especially in the VOD, the applicability of the assumptions and the accuracy of the parameter values in the estimation formulas. Still, the estimation accuracy has been improved compared to other empirical formulas shown in Table 7.

Table 8: Estimations of the borehole pressures in the test shots using the new formula

Test No.	Charge diameter (mm)	Borehole diameter (mm)	Explosion pressure, P_e* (GPa)	Borehole pressure, P_{bc}		
				Estimation (GPa)	Measured (GPa)	Error
1	16	38	0.48	0.085	**0.08**	+6%
2	16	38	0.70	0.12	**0.12**	0%
3	21.2	38	0.83	0.26	**> 0.6**	> -57%
4	21.2	38	0.95	0.30	**0.81**	-63%

*: The values of P_e were taken as the average estimation of P_e in Table 6.

3.3 Measured duration of the borehole pressure

The measured pressure period lasts from 30 to 500 μs. The factor that determined the signal period is the cable from the sensor through the bottom of the LHM cup.

When the LHM gage is placed upon a cable hole and beneath the explosive as in Fig. 5a, the pressure from the detonating explosive forces the LHM cup into the cable hole. The bottom of the LHM cup is compressed, squeezes the cable inside, causes at first a short-circuit in the cable and then cuts off the cable. The photos of the recovered LHM cups after the blasting experiments are good evidences to this process, see photos in Figs. A7-b, A8-b and A9-b in Appendix IV.

In one shot where the LHM cup was placed upside-down on the explosive, see Fig. 5b, the cup was expanded by the inside pressure to such an extent that the cup was held in place by the friction between the borehole wall and the cup, while the bottom of the cup was blown away, see photo in Fig. A10-b in Appendix IV. The cable was probably damaged (cut) long before the bottom was blown away.

According to Eq. 7, a short-circuit in the cable causes the resistance in the circuit $R = 0$ and the corresponding pressure $P = +\infty$, which is a positive overflow in the pressure history. On the other hand, a cut-off of the cable results in $R = \infty$ and $P = 0$, which is a sudden pressure drop to zero in the pressure history.

As can be seen in Figs. 6 and 7, all pressure histories were terminated by either a short-circuit or a cut-off of the cable. The measured durations of the borehole pressure were short for this reason. Had the damage to the cable been less or occurred later, the measured pressure durations would have been longer. Therefore, protection of the cable is the only solution to achieve longer recording durations.

Efforts have been made to fill the cable hole and the gap between the cup and the blast hole wall with a chemical grouting material. A filling method has been developed and worked very well, see Appendix V. It is believed that the grouting material would, after hardening, be strong enough to protect the LHM cup and the cable for a sufficiently long period for measurement. However, during the experiments, the temperature in the quarry was around -5 °C and the grouting material never hardened. Neither has any cable protection been achieved.

3.4 Analysis of the performance of the LHM gage

Generally speaking, the LHM gage worked very well. In the following, details in the recorded signals as exemplified in Fig. 11 will be described.

Noise from the detonating explosive: It has been observed that spurious signals have been recorded prior to the pressure arrival to the gage, see Figs. 6 and 7 or Appendix IV. A closer examination of the arrival time revealed that this noise appeared in the record simultaneously with the detonation in the explosive. That is to say, the noise was recorded as soon as the explosive was initiated by the detonator located approximately 0.6 m away from the LHM gage. And the noise disappeared when the detonation ended. Thus, this noise must be a form of electromagnetic phenomenon generated by the detonating explosive, since no other mechanic waves could propagate so rapidly. For example, a P-wave would take approximately 0.12 ms to propagate from the detonator to the LHM gage, assuming the P-wave velocity in the granite to be 5000 m/s.

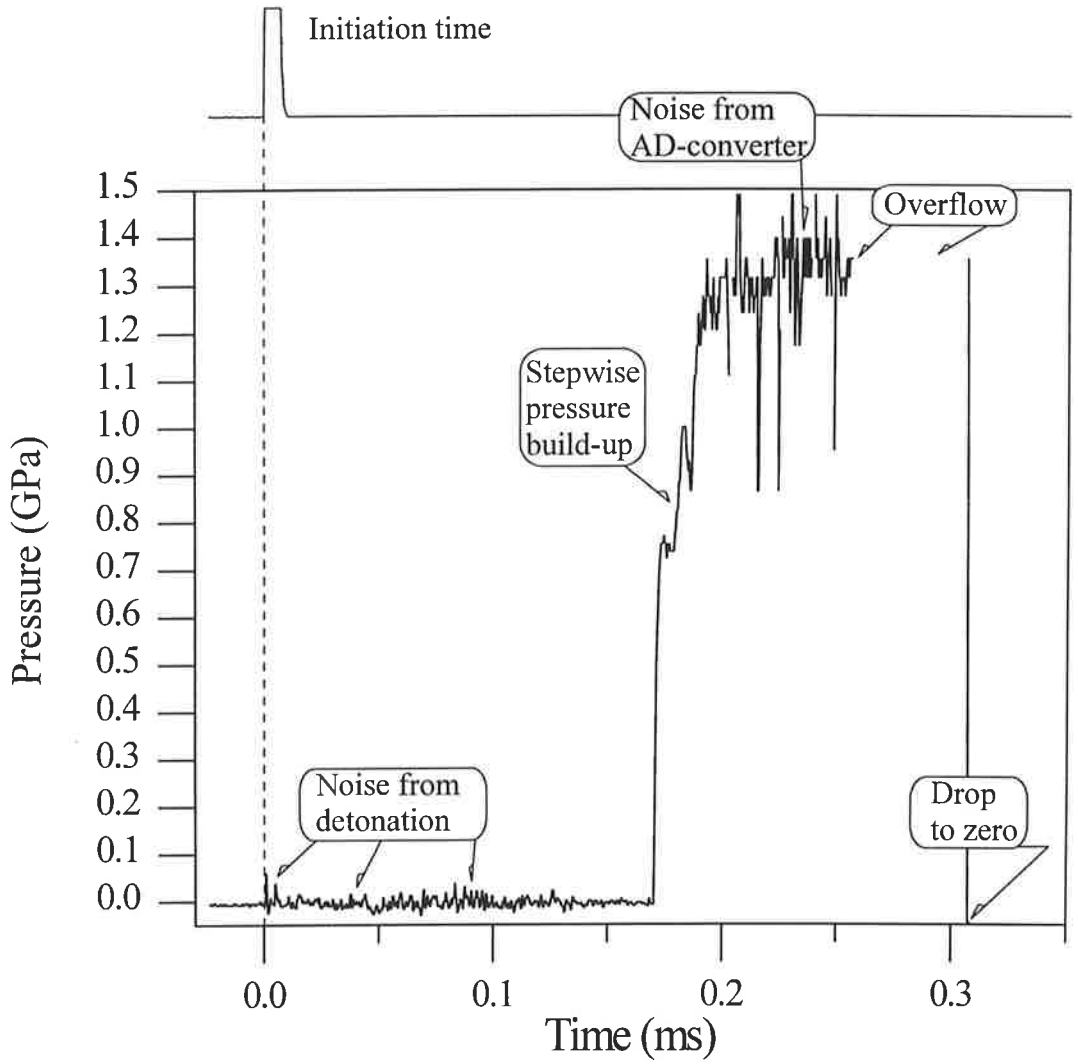

Fig. 11: Some details in the recorded signals. The signal displayed here is from Test No. 5.

This electromagnetic phenomenon from the detonating explosive has been eliminated by grounding the LHM cup to the ground of the whole measuring system. In the very first shot, the LHM cup was not grounded and the noise from the detonating explosive distorted severely the pressure history, see the left uppermost signal in Fig. 6 or Fig. A4 in Appendix IV. After that, the LHM cup was always grounded, as shown in Fig. 2, which protected the measurements from the electromagnetic noise.

Stepwise build-up of pressure: On the upstream side of the pressure history, one can see two to three steps of the pressure increase. These steps resulted from the collisions of waves at the sensor. Since the sensor is located 12.5 mm above the bottom of the LHM cup, see Fig. 2, the shock waves are reflected at the bottom of the LHM cup, after the

waves pass the sensor and then collide with the incident shock waves. In the earlier laboratory experiments /4/, these wave collisions were also clearly observed and the shock wave velocity in the water has been determined in this way to be 1600 to 1800 m/s. In this study in stone blocks, the shock wave velocity in water has been determined to be 1250 ~ 3000 m/s depending on the pressure amplitude, see Table 4.

Overflow and sudden pressure drop to zero: Both overflow and sudden pressure drop to zero can be seen in the pressure histories in Figs. 6 and 7. These phenomena were caused by the short-circuit in respective cut-off of the cable passing through the bottom of the LHM cup, as described in Section 3.3.

4 CONCLUSIONS

The following conclusions can be drawn based on the analysis of the pressure measurements in seven blast holes in stone blocks.

- The LHM method worked very well and good pressure signals have been obtained.
- It is necessary to ground the LHM cup to avoid the electromagnetic noises from the detonating explosive.
- The signal cable from the LHM cup determines the measured pressure duration. It is believed that a better protection of this cable by e.g. grouting material will result in longer signal durations.
- A number of empirical formulas for detonation pressure, explosion pressure and borehole pressure in decoupled holes have been collected. The predictions of those formulas have been compared with the measurements.
- The estimates of detonation pressure by six formulas did not differ much from each other, within ±12% around the average.
- The estimates of explosion pressure by five formulas differed within ±17% around the average and the agreement with two measured explosion pressures is rather good.
- Two formulas for borehole pressure in decoupled holes have been compared to the measurements. The agreement between the estimates and the measurements is generally very poor with estimation error from -11% to -75%. Nevertheless, when decoupling ratio is large, 2.375, Calder's formula provided good estimates, error within -14%.
- A new estimation principle for borehole pressure in decoupled holes has been proposed. According to this principle, the borehole pressure in a decoupled hole is estimated by the explosion pressure in a blast hole, in which a "Spread Charge" is charged. The "Spread Charge" is an explosive which has the same composition and quantity as the explosive charged in a decoupled hole. However, its lower density makes it fully and uniformly fill the blast hole instead of being concentrated in (the central) part of the hole.
- The estimation accuracy of the new formula is better than the existing formulas. However, it is still not good enough for the holes with small decoupling ratio.

ACKNOWLEDGEMENT

The author gratefully acknowledge Junhua Deng at SveBeFo for his assistance in the measurements in field and Bo Alexandersson at Göinge Stenförädlning AB for his efforts in transporting blocks, drilling holes and arranging practical issues for the field tests.

REFERENCES

1. Ouchterlony F: "Prediction of Crack Lengths in Rock after Cautious Blasting with Zero Inter-hole Delay". FRAGBLAST - International Journal for Blasting and Fragmentation, Vol. 1, No. 4, 1997.

2. Olsson M and Bergqvist I: "Crack Propagation in Rock from Multiple Hole Blasting". SveBeFo Report 18, 1995. (In Swedish).

3. Hustrulid W et al: "A New Method for Predicting the Extent of the Blast Damage Zone". Proc. of Blasting Conference, Paper No. 3, Nitro Nobel, Gyttorp, 1992.

4. Persson G: "LHM, a Method for Measurement of the Entire Pressure History in Blast Holes". SveBeFo Report 34. 1999. (In Swedish)

5. Rustan A: "Rock Blasting Terms and Symbols". A A Balkema/Rottersam/Brookfield. 1998.

6. Zerill F J (Editor): "Notes from Lectures on Detonation Physics". NSWC MP 81-399. Naval Surface Weapons Center, Silver Spring, Maryland 20910. Oct., 1981.

7. Literature about the manganin can be found in many of the Detonation Symposium Proceedings. The following is an example.
   Song S Y and Lee J W: "A Detonation Pressure Measurement System Employing High Resistance Manganin Foil Gauge". 9th Symp. on Detonation, pp. 471. Portland, Oregon. Aug. 28 - Sept. 1, 1989.

8. Davies F W, Smith E A and De La Cruz C: "The Measurement of Detonation Waves in Composite Explosives". Proc. of 13th Annual Symp. on Explosives and Blasting Research, pp. 145. Las Vegas, Nevada. Feb. 2-5, 1997.

9. Watson R: "Gauge for Determining Shock Pressure". The Review of Scientific Instruments, Vol. 38, No. 7, pp. 978. Jul., 1967.

10. Wieland M: "Cross Borehole Stress Wave Measurements in Underground Coal". Proc. of 4th Mini-Symp. on Explosives and Blasting Research, pp. 16. Anaheim, California. Feb. 4-5, 1988.

11. Katsabanis P D and Yeung C: "Effects of Low Amplitude Shock Waves on Commercial Explosives, The Sympathetic Detonation Problem". Proc. of 14th International Symp. on Rock Fragmentation by Blasting - FRAGBLAST-4, pp. 401. Vienna, Austria. Jul. 5-8, 1993.

12. Wilson W H, Holloway D C and Bjarnholt G: "Measurement of Pressure Loadings from Explosively Loaded Boreholes used Expendable Piezoresistive Transducers". Proc. of 1987 American Society of Mechanical Engineers Meeting, pp. 97. Cincinnati, Ohio. Jun. 14-17, 1987.

13. Ginsberg M J and Asay B W: "Commercial Carbon Composition Resistors as Dynamic Stress Gauges in Difficult Environments". Rev. Sci. Instrum. 62 (9), pp. 2218-2227. Sept. 1991.

14. Fried L E: "Cheetah 1.39 User's Manual". Lawrence Livermore National Laboratory, UCRL-MA-117541 Rev. 3. March 19, 1996.

15. Calder P: "Pit Slope Manual, Chapter 7 - Perimeter Blasting". CANMET (Canadian Center for Mineral and Energy Technology) Report 77-14. May, 1977.

16. Ouchterlony F: "Prediction of Crack Lengths in Rock after Cautious Blasting with Zero Inter-Hole Delay". SveBeFo Report 31, 1997.

17. Atlas Powder: "Explosives and Rock Blasting". Atlas Powder Company, Dallas, Texas, USA. 1987.

18. Deng J et al: "A Burning Model for Five Emulsion Explosives and Its Applications". SveBeFo Report 43. 1999.

APPENDIX I: Empirical formulas for estimation of detonation pressure, explosion pressure and borehole pressure

There are a number of empirical formulas collected in this Appendix for estimation of detonation pressure, explosion pressure and borehole pressure. However, keep in mind that each formula may be developed under certain specific conditions and may not be applied universally. Definition of these different pressures can be found in Section 1.1.

Following symbols are defined:

D = velocity of detonation or VOD (m/s)
D_∞ = ideal VOD (m/s)
e_0 = internal energy of the explosive (J)
L_b = length of the blast hole (m)
L_e = length of the charge in a blast hole (m)
P = pressure (Pa)
P_0 = ambient pressure (Pa) = 1 atm.
P_b = borehole pressure in a decoupled blast hole (Pa)
$P_b = P_e$ in a fully charged hole
P_{CJ} = detonation pressure (Pa)
P_e = explosion pressure (Pa)
q = heat of detonation (J/kg)
r_b = radius of the blast hole (m)
r_e = radius of the charge in a blast hole (m)
S = entropy (J)
u_{pCJ} = particle velocity at the CJ state (m/s)
v = volume (m^3)
v_b = volume of the blast hole (m^3)
v_e = volume of the charge (m^3)
γ = adiabatic coefficient = $-(\partial \ln p/\partial \ln v)_s$
γ_{CJ} = γ at the CJ state
ρ_0 = density of the unreacted explosive (kg/m^3 or otherwise specified)

1 Detonation pressure, P_{CJ}

The conservation of momentum in a detonation means:

$$P_{CJ} = \rho_0 u_{pCJ} D + P_0 \qquad \text{(A1)}$$

At the CJ state, the following relation exists:

$$u_{pCJ} = D/(1+\gamma_{CJ}) \qquad \text{(A2)}$$

Combing Eqs. A1 with A2 and taking into account that P_0 is negligible compared with P_{CJ}, Eq. 1 becomes:

$$P_{CJ} = \rho_0 D^2/(1+\gamma_{CJ}) \qquad \text{(A3)}$$

Here, ρ_0 and D can be easily measured with very good accuracy. If γ_{CJ} is known, the detonation pressure, P_{CJ}, can be calculated readily from Eq. A3. Therefore, there exist two kinds of empirical formulas for P_{CJ}. One is the empirical formula for direct estimation of P_{CJ}. The other is Eq. A3 combined with an empirical formula for γ_{CJ}.

In the following, one empirical formula for P_{CJ} and six empirical formulas for γ_{CJ} are presented.

Formula 1: according to Zhou and Yu /A1/, for a high explosive having a chemical formula of $C_aH_bN_cO_d$ ($0.5b \le d \le 2a+0.5b$):

$$P_{CJ} = (1.60G + 1.945)^2\rho_0^2 \quad \text{(A4)}$$

Here: ρ_0 in g/cm^3

$$G = \frac{0.5b + c + d}{2a + b + c} \quad \text{(A5)}$$

Formula 2: according to Kamlet and Jacobs /A2/, Kamlet and Dickinson /A3/, Kamlet and Hurwitz /A4/ and Kamlet and Short /A5/, for ideal CHNO and CHNOF explosives at loading density exceeding 1 g/cm^3:

$$\gamma_{CJ} = 0.655/\rho_0 + 0.702 + 1.107\rho_0 \quad \text{(A6)}$$

Here: ρ_0 in g/cm^3

Formula 3: according to Defourneaux /A6/, for a CHNO high explosive:

$$\gamma_{CJ} = 1.9 + 0.6\rho_0 \quad \text{(A7)}$$

Here: ρ_0 in g/cm^3

Formula 4: assuming that the detonation is ideal and the detonation gases follow the polytropic gas law /A7/:

$$\gamma_{CJ} = \sqrt{1 + \frac{D_\infty^2}{2(q + e_0)}} \quad \text{(A8)}$$

Formula 5: according to Wu /A8/, for a high explosive having a chemical formula of $C_aH_bN_cO_d$:

$$\gamma_{CJ} = 1.25 + \gamma_0\left(1 - e^{-0.546\rho_0}\right) \quad \text{(A9)}$$

Here: ρ_0 in g/cm^3 and

$$\gamma_0 = \frac{0.5b + c + d}{0.0482a + 0.446b + 0.2632c + 0.298d} \quad \text{when d-½b-2a} \ge 0 \quad \text{(A10a)}$$

$$\gamma_0 = \frac{a + 0.43b + 0.5c}{0.2857a + 0.2549b + 0.1316c + 0.018d} \quad \text{when d-½b-2a} < 0 \quad \text{(A10b)}$$

$$\gamma_0 = \frac{a + 0.35b + 0.5c}{0.2857a + 0.2166b + 0.1316c + 0.018d} \quad \text{when d-½b-a} \le 0 \quad \text{(A10c)}$$

$$\gamma_0 = \frac{a + 0.5b + 0.5c - 0.46d}{0.2857a + 0.147b + 0.1316c + 0.081d} \quad \text{when d-½b} \le 0 \text{ and } a \ge d \quad \text{(A10d)}$$

$$\gamma_0 = \frac{a + 0.5b + 0.5c}{0.0734a + 0.147b + 0.1316c + 0.3d} \quad \text{when d-½b} \le 0 \text{ and } a < d \quad \text{(A10e)}$$

Formula 6: for high explosive with $\rho_0 = 1 \sim 1.8$ g/cm^3 /A9/:

$$\gamma_{CJ} \approx 3 \quad \text{(A11)}$$

Formula 7: according to Cooper /A9/:

$$\gamma_{CJ} = 1/(1.4035\rho_0^{-0.04} - 1) \quad \text{(A12)}$$

Here: ρ_0 in g/cm^3

2 Explosion pressure or the borehole pressure in a fully charged blast hole, P_e

If the expansion of the detonating explosive from the C-J plane to the original explosive volume is assumed to obey the polytropic gas equation of state (EOS) or the γ-law EOS with a constant γ value, then the explosion pressure is exactly a half of the detonation pressure /A7/, i.e.

$$P_e = \tfrac{1}{2} \cdot P_{CJ} \quad \text{(A13)}$$

Besides this, further three empirical formulas are presented below.

Formula 1: according to Calder /A10/:

$$P_e = N(\rho_0)\, \rho_0\, D^2 \quad \text{(A14)}$$

Here: $N(\rho_0)$ = a coefficient varying with ρ_0 /A10/

$= 0.235(\rho_0/1000)^{-0.57} - 0.08$ for $800 \le \rho_0 \le 2000$ /A11/

Formula 2: Gulf Oil Chemicals Company formula /A12/:

$$P_e = 0.1125\, \rho_0\, D^2 \quad \text{(A15)}$$

Formula 3: according to Sanchidrian et al. /A13/:

$$P_e = 228\, \rho_0\, D^2/(1+0.8\rho_0) \quad \text{(A16)}$$

Here: ρ_0 in g/cm^3

Formula 4: according to Ouchterlony /A11/:

$$P_e = \gamma^\gamma/(\gamma+1)^{(\gamma+1)} \cdot \rho_0\, D^2 \quad \text{(A17)}$$

Here: $\gamma = \gamma_{CJ}$ and is calculated by Eq. A8.

This formula actually approximates P_e by the pressure at $v = v_0$ on the expansion isentrope from P_{CJ}: Pv^γ = constant, where γ is a constant.

3 Borehole pressure in a decoupled blast hole, P_b

Assuming that a) the expansion of the detonating explosive from the original explosive volume to the borehole volume is an isentropic process and b) the adiabatic gamma (γ) is a constant during the entire expansion, then the relation between the borehole pressure

in a fully charged blast hole, P_e, and in a decoupled blast hole, P_b, can be reduced, as described below.

$$\gamma = -\left(\frac{\partial \ln P}{\partial \ln v}\right)_S = \text{constant}$$

can be transformed to

$$Pv^{\gamma} = \text{constant} \tag{A18}$$

Applying Eq. A18 to the expansion in a blast hole from P_e to P_b:

$$P_e v_e^{\gamma} = P_b v_b^{\gamma} \tag{A19}$$

That is:

$$P_b = P_e \cdot \left(\sqrt{\frac{L_e}{L_b}} \cdot \frac{r_e}{r_b}\right)^{2\gamma} \tag{A20}$$

It is difficult to assign an adequate γ value to this equation, since γ is really not a constant in the reality. It varies, among other factors, with the species of the detonation gases. However, it is known that when the detonation gases are expanded into a very large volume, approximately 20 times the original explosive volume, γ approaches a value of 1.2 to 1.3.

These two γ values, namely 1.2 and 1.3, have been used in empirical formulas as in Eqs. A20a and A20b.

$$P_b = P_e \cdot \left(\sqrt{\frac{L_e}{L_b}} \cdot \frac{r_e}{r_b}\right)^{2.4} \tag{A20a}$$

Here, P_e is calculated by Eq. A14, according to Workman and Calder /A14/.

$$P_b = P_e \cdot \left(\sqrt{\frac{L_e}{L_b}} \cdot \frac{r_e}{r_b}\right)^{2.6} \tag{A20b}$$

Here: $P_e = \rho_0 D^2/8$, according to Atlas Powder /A15/.

References

A1. Zhou X X and Yu Y Z: "Estimation of Detonation Velocity and Detonation Pressure for CHNO Explosive Mixtures". Journal of the Industrial Explosives Society, Japan. Vol. 53, No. 1, pp 8-12. Jan. - Feb. 1992.

A2. Kamlet M J and Jacobs S J: "Chemistry of Detonations. I. A Simple Method for Calculating Detonation Pressures of C-H-N-O Explosives". J. Chem. Phys. 48, 23, 1968.

A3. Kamlet M J and Dickinson C: "Chemistry of Detonations. III. Evaluation of the Simplified Calculational Method for Chapman-Jouguet Detonation Pressures on the Basis of Available Experimental Information". J. Chem. Phys. 48, 43, 1968.

A4. Kamlet M J and Hurwitz H: "Chemistry of Detonations. IV. Evaluation of a Simple Predictional Method for Detonation Velocities of C-H-N-O Explosive". J. Chem. Phys. 48, 3685, 1968.

A5. Kamlet M J and Short J M: "Chemistry of Detonations. VI. A Rule for Gamma as a Criterion for Choice among Conflicting Detonation Pressure Measurements". Combustion and Flame, 38, 221. 1980.

A6. Defourneaux M: "Sciences of Techniques de L'armement". pp 872. 1973.

A7. Zerill F J (Editor): "Notes from Lectures on Detonation Physics". NSWC MP 81-399. Naval Surface Weapons Center, Silver Spring, Maryland 20910. Oct., 1981.

A8. Wu X: "A Simple Method for Calculating Detonation Parameters of Explosives". J. Energetic Materials. Vol. 3, pp 263-277, 1985.

A9. Cooper P W: "Explosives Engineering". VCH Publishers, Inc. 1997.

A10. Calder P: "Pit Slope Manual, Chapter 7 - Perimeter Blasting". CANMET (Canadian Center for Mineral and Energy Technology) Report 77-14. May, 1977.

A11. Ouchterlony F: "Prediction of Crack Lengths in Rock after Cautious Blasting with Zero Inter-Hole Delay". SveBeFo Report 31, 1997.

A12. Neil E G: "The Future of Slurry Explosives". Proc. 8th Conf. on Explosives and Blasting Technique, Society of Explosives Engineers Annual Meeting. New Orleans, Louisiana. pp 217-228. 1982.

A13. Sanchidrián J A et al.: "Improvement of Productivity in Quarrying Dimension Stone Using New Drilling and Blasting Techniques". Paper Presented at Brite-Euram Workshop on Ornamental Stones, Montpellier. Sept. 30, 1996.

A14. Workman J L and Calder P N: "A Method for Calculating the Weight of Charge to Use in Large Hole Presplitting for Cast Blasting Operations". Proc. 17th Conf. on Explosives and Blasting Technique, Society of Explosives Engineers. Las Vegas, Nevada. pp 97-108. 1991.

A15. Atlas Powder: "Explosives and Rock Blasting". Atlas Powder Company, Dallas, Texas, USA. 1987.

APPENDIX II: Measurements of VOD and charge density of Gurit B cartridges.

A series measurements of VOD have been carried out on unconfined Gurit B cartridges. Four cartridge sizes with nominal outer diameters of 17, 22, 39 and 51 mm have been planned. However, during the experiment, Gurit B cartridges in ϕ 17 mm and ϕ 51 mm were not available. Thus, cartridges of these two sizes were packed by ourselves with the explosive taken from ϕ 22 mm and ϕ 39 mm cartridges. Charge density are strictly controlled during the packing.

The measured parameters in the experiments are: outer and inner diameters of the plastic cartridge, charge density, charge length and VOD. Test results are summarized in Table A1.

Two methods were used for the measurements of VOD: one is the ionisation method and the other is a continuous method based on a resistance wire, see Appendix III.

The ionisation method was used for ϕ 22, ϕ 39 and ϕ 51 mm cartridges. Three measuring points or two measuring distances were monitored in each cartridge.

Table A1: Measurements of VOD and density of unconfined Gurit B cartridges

Cartridge diameter		Charge length (mm)	Charge density (kg/m^3)	VOD measurement					
Inner * (mm)	Outer (mm)			ΔL (mm)	Δt_1 (μs)	$\Delta L/\Delta t_1$ (m/s)	Δt_2 (μs)	$\Delta L/\Delta t_2$ (m/s)	**Mean VOD (m/s)**
16.0	17.0	455	1120	N.A					**2167**
16.0	17.0	455	1120	N.A					**2288**
16.0	17.0	455	1120	N.A					**2185**
16.0	17.0	455	1120	N.A					**1967**
21.2	22.5	1050	1050	50	—	—	214.0	2336	**2336**
21.2	22.5	1050	1050	20	85.5	2339	73.4	2725	**2532**
21.2	22.5	1050	1050	20	89.1	2245	83.7	2389	**2317**
21.2	22.5	1050	1050	20	87.4	2288	83.2	2404	**2346**
37.6	39.0	1110	1050	49	—	—	156.0	3141	**3141**
37.6	39.0	1110	1050	20	66.9	2990	66.6	3003	**2997**
37.6	39.0	1110	1050	20	65.9	3035	65.2	3067	**3051**
37.6	39.0	1110	1050	20	68.5	2920	67.0	2985	**2953**
49.2	51.0	1050	1050	20	59.6	3356	57.7	3466	**3411**
49.2	51.0	1050	1050	20	59.1	3384	57.8	3460	**3422**
49.2	51.0	1050	1050	20	59.7	3350	59.0	3390	**3370**

*: Inner cartridge diameter = charge diameter.
N.A: Not applicable, since VOD was measured with the continuous method.

The continuous method was used for ϕ 17 mm cartridge. However, the detonation in this cartridge size is too weak to short-circuit the resistance wire. From the records, only two

points could be identified clearly: the initiation of the charge by the detonator and when the detonation reached the end of the charge, see Fig. A1 as an example. Therefore, the VOD in this cartridge size was calculated from the above-mentioned two points. Or, the VOD value here is the average VOD over the whole charge length.

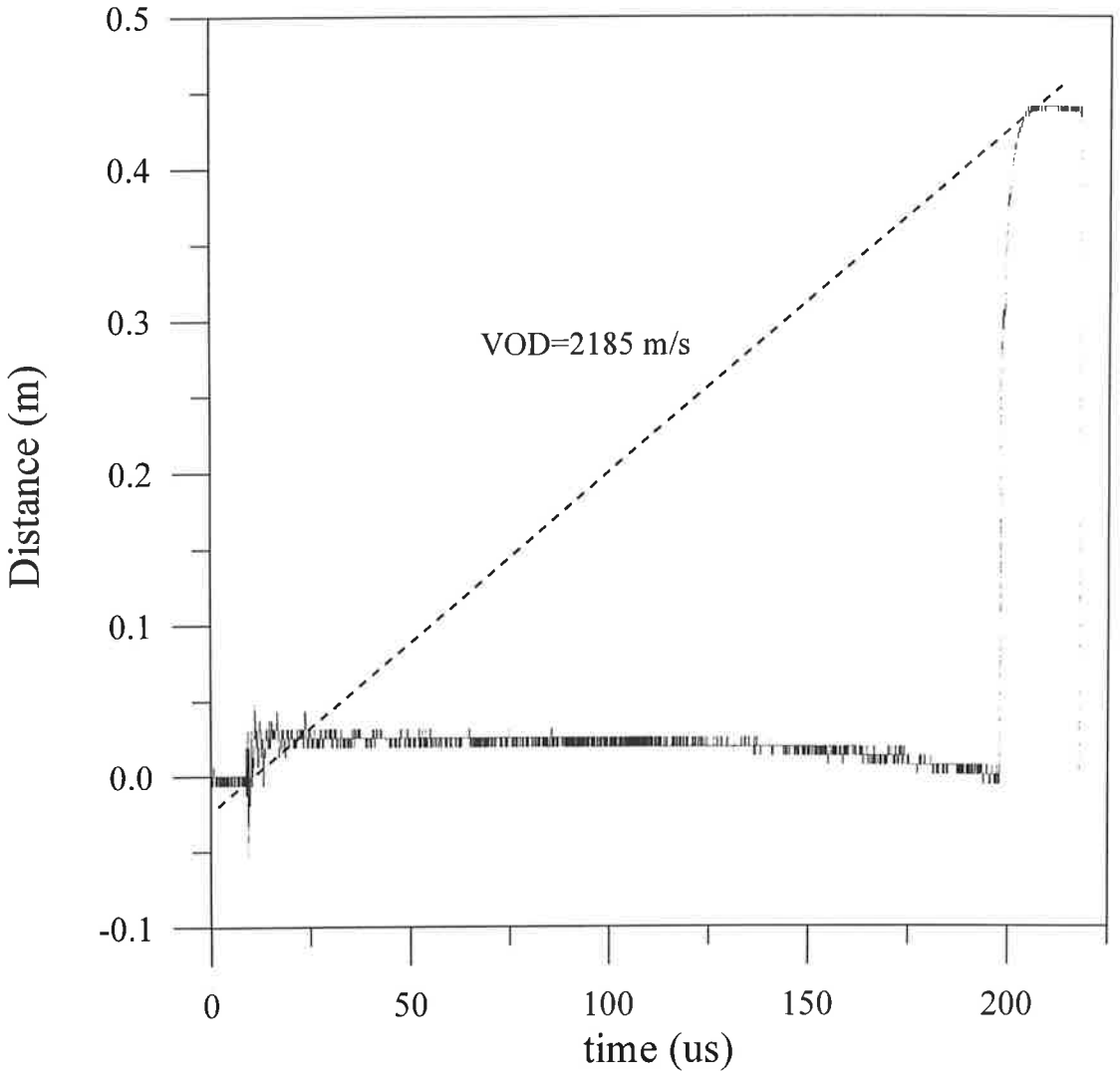

Fig. A1: An example of the signal from the continuous measurement of VOD in ϕ 17 mm Gurit B cartridge.

Based on the results in Table A1, a regression line can be drawn for VOD versus inverse charge diameter, see Fig. A2, and the expression of the regression line is:

$$VOD = 3857 - 28674/d \quad (A21)$$

where: VOD = VOD of Gurit B (m/s)
d = charge diameter of Gurit B (mm)

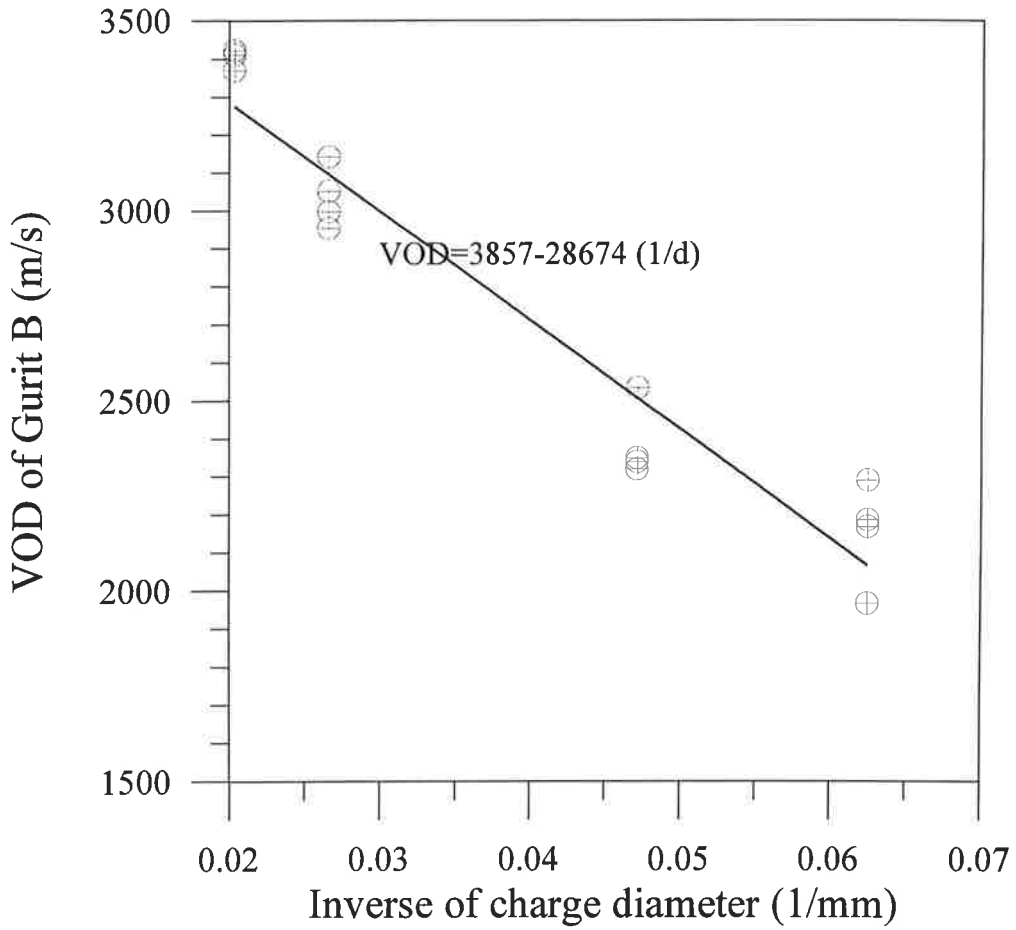

Fig. A2: VOD in unconfined Gurit B cartridges versus inverse of the charge diameter.

APPENDIX III: Method to measure VOD continuously based on a resistance wire, a constant-voltage power source and an oscilloscope.

In order to utilise the existing equipment at SveBeFo and the commercially available resistance wires for the purpose of continuous measurement of VOD, a measuring system has been designed. Laboratory tests have proven that the system is reliable and quite easy to use. Furthermore, the system is also flexible, e.g. the sampling rate can be easily adjusted by the oscilloscope or other recording equipment.

1 Measuring system

The scheme of the measuring system is illustrated in Fig. A3, where a two-lead resistance wire is inserted inside or fasten on the explosive charge to be measured. As the detonation propagates, it short-circuits the resistance wire, reduces its resistance and results in a voltage increase over the shunting resistance R_1. This voltage increase may be recorded by a tape recorder, memory oscilloscope or other recording devices. We use a LeCroy digital oscilloscope.

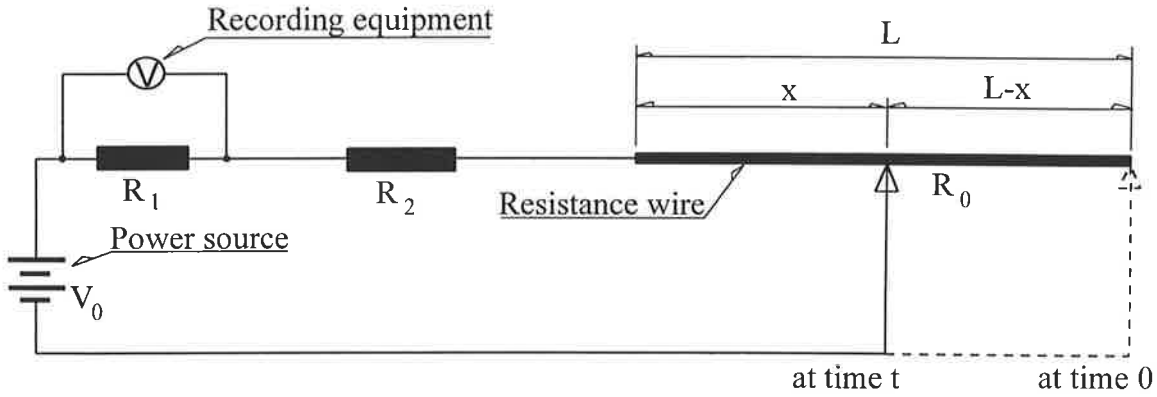

Fig. A3: Scheme of the measuring system for continuous VOD measurement. In the scheme, V_0 = the voltage of the constant-voltage source; L = original charge length; x = remaining charge length at time t; L-x = length of the detonated charge at time t; R_0 = resistance of the wire to be consumed by the detonation; R_1 = shunting resistance; R_2 = rest of resistance in the circuit e.g. cable resistance and rest resistance in the wire after the detonation; "Time 0" = the moment of initiation; "Time t" = time t after the initiation.

2 Data analysis

The following data process is necessary to calculated the VOD from the measured voltage increase.

Assigning V as the voltage over the shunting resistance R_1 and c ($c = R_0/L$) is the unit resistance in the wire, then, relations in Table A2 can be established.

Table A2: Relations between the measured voltage and the resistances in the circuit.

Time	Resistance in the wire (Ω)	Voltage over R_1 (V)
At the initiation moment	R_0	$V_{min} = \frac{R_1}{R_0 + R_1 + R_2} \cdot V_0$ (A22)
At the end of detonation	0	$V_{max} = \frac{R_1}{R_1 + R_2} \cdot V_0$ (A23)
At any time during the detonation	c·x	$V(t) = \frac{R_1}{R_1 + R_2 + c \cdot x} \cdot V_0$ (A24)

According to Eq. A24, the remaining charge length, x, is:

$$x = \frac{V_0 \cdot R_1}{c} \cdot \frac{1}{V(t)} - \frac{R_1 + R_2}{c} \tag{A25}$$

Thus, the VOD can be calculated as:

$$VOD = -\frac{dx}{dt} = \frac{V_0 \cdot R_1}{c} \cdot \frac{1}{V(t)^2} \cdot \frac{dV(t)}{dt} \tag{A26}$$

However, since the V(t) signals are not always as smooth as desired and Eq. A26 is quite sensitive to the noise, we seldom use this equation for the VOD calculation. Instead, we use Eq. A25 and plot x versus t in a diagram (see Fig. A1 as an example), make a regression and find the VOD values.

3 Optimization of the shunting resistance

The shunting resistance (R_1) should be adjusted according to the initial resistances in the measuring circuit (R_0 and R_2) in order to enhance the resolution of the output.

The best resolution is achieved when the difference between the voltages over R_1 before and after the detonation is maximum, i.e. when $|V_{min} - V_{max}|$ reaches the maximum. Therefore, this is required:

$$\frac{d|V_{min} - V_{max}|}{dR_1} = 0 \tag{A27}$$

According to Eqs. A22 and A23:

$$\left|V_{min}-V_{max}\right|=\left|\frac{1}{R_0+R_1+R_2}-\frac{1}{R_1+R_2}\right|\cdot V_0\cdot R_1 \qquad \text{(A28)}$$

Inserting Eq. A28 into Eq. A27 results in:

$$R_1^2+R_2^2+R_0\cdot R_2=0 \qquad \text{(A29)}$$

Or:

$$R_1=\sqrt{R_2\cdot(R_0+R_2)} \qquad \text{(A30)}$$

We adjust both R_1 and the zero-shift level of the input channels in the oscilloscope and obtain very good resolution.

APPENDIX IV: Signals from borehole pressure measurements in seven stone blocks and photos of the LHM cups recovered after the blasting experiments.

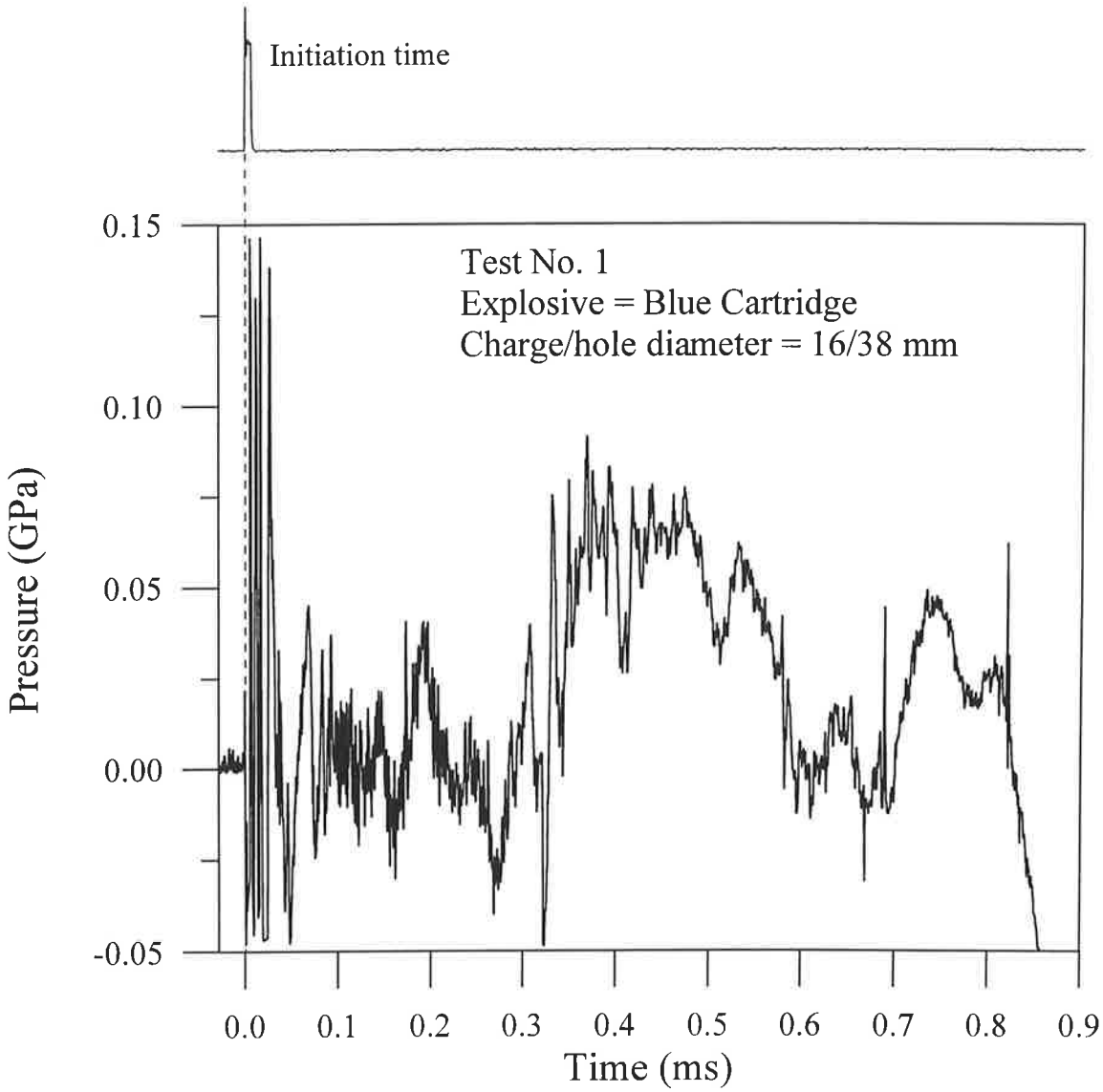

Fig. A4: Measured borehole pressure. Test No. 1. The LHM cup before and after the blast can be seen in Fig. A5-b.

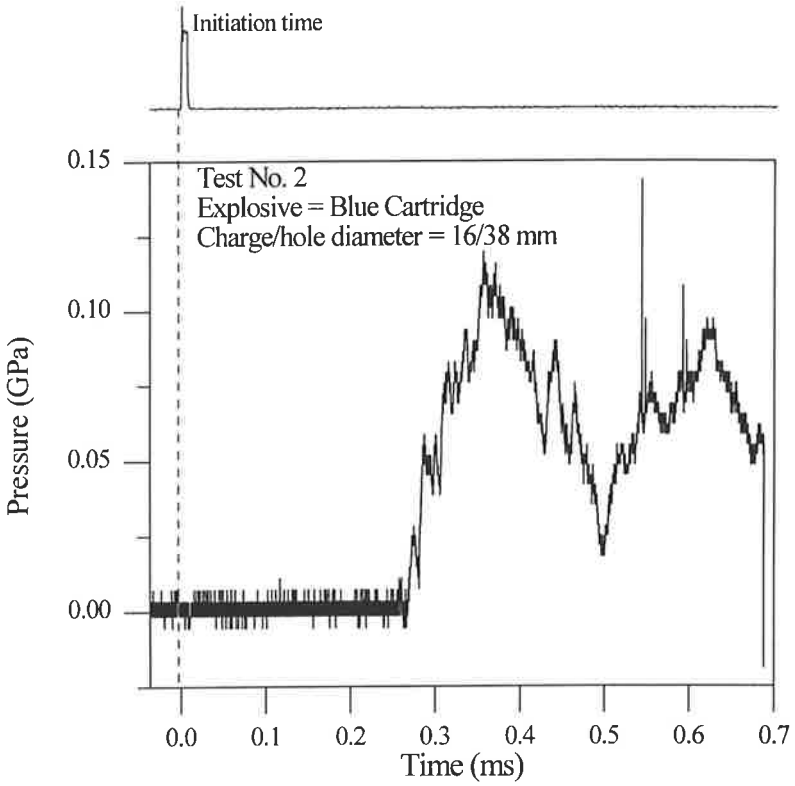

Fig. A5-a: Measured borehole pressure. Test No. 2. The LHM cup before and after the blast can be seen in Fig. A5-b.

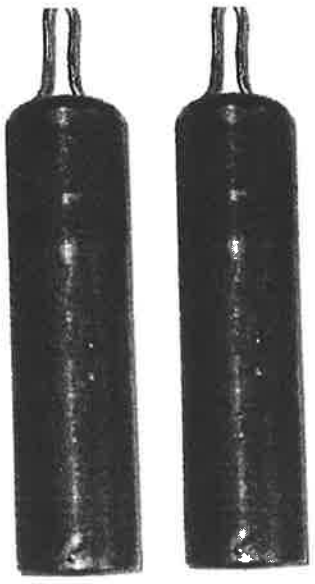

Fig. A5-b: The LHM cup before and after the blasting experiments in Tests No. 1 and No. 2. No damage or deformation has occurred to the cup in these two test shots.

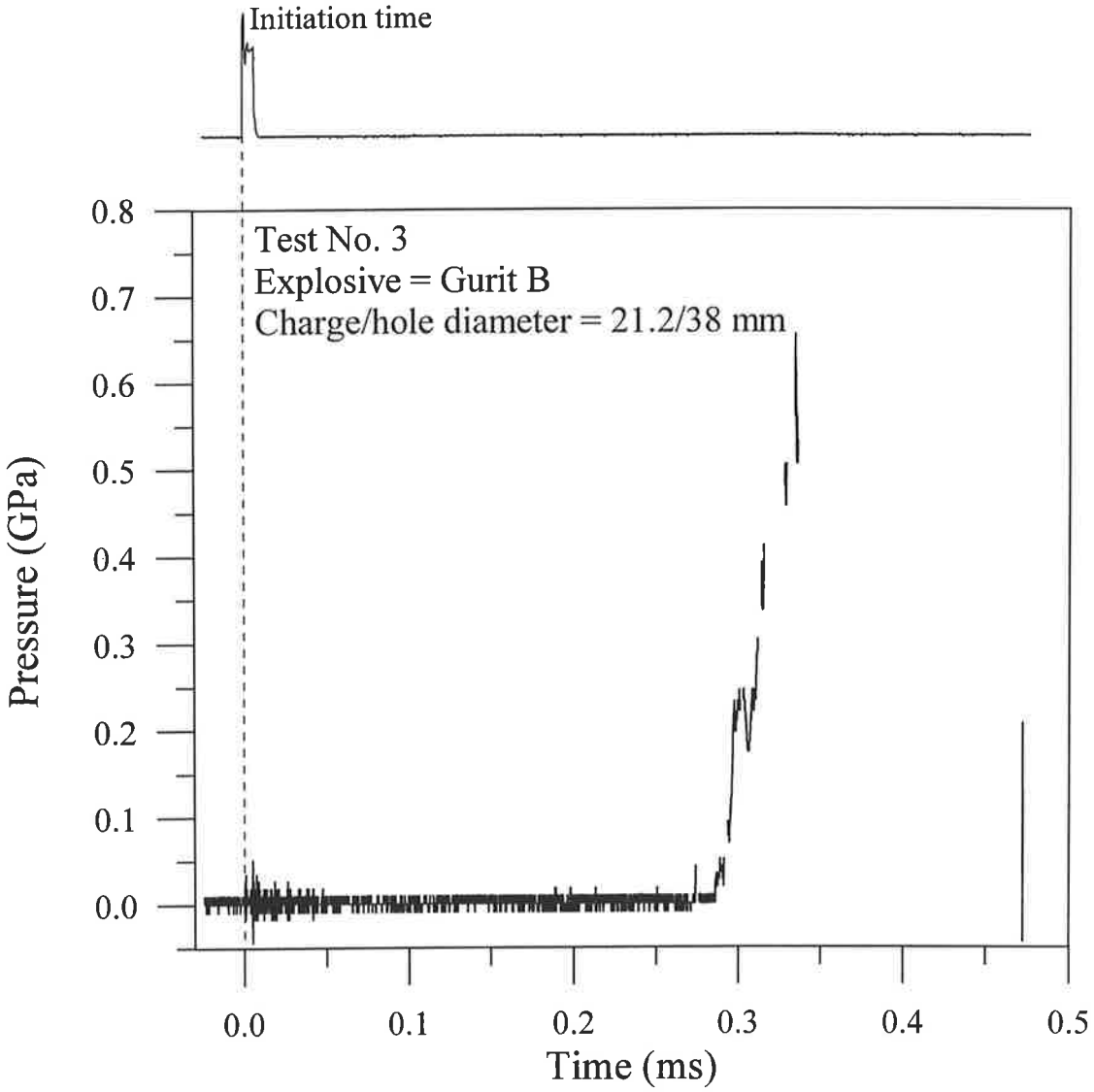

Fig. A6: Measured borehole pressure. Test No. 3. The LHM cup before and after the blast can be seen in Fig. A7-b.

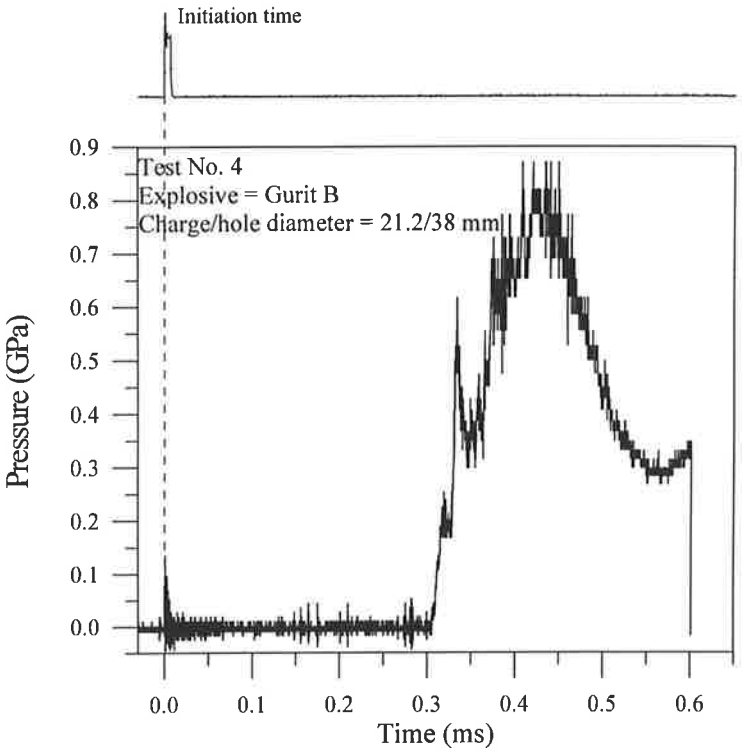

Fig. A7-a: Measured borehole pressure. Test No. 4. The LHM cup before and after the blast can be seen in Fig. A7-b.

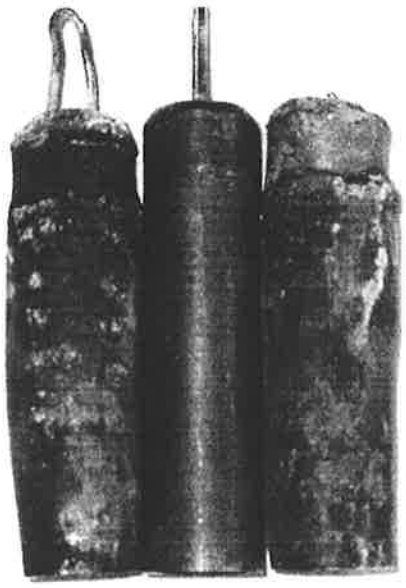

Fig. A7-b: The LHM cup before and after the blasting experiments in Tests No. 3 and No. 4. The bottom part of the cup was diminished when it was squeezed into the cable hole by the pressure. The rest of the cup was swelled by the pressure inside it.

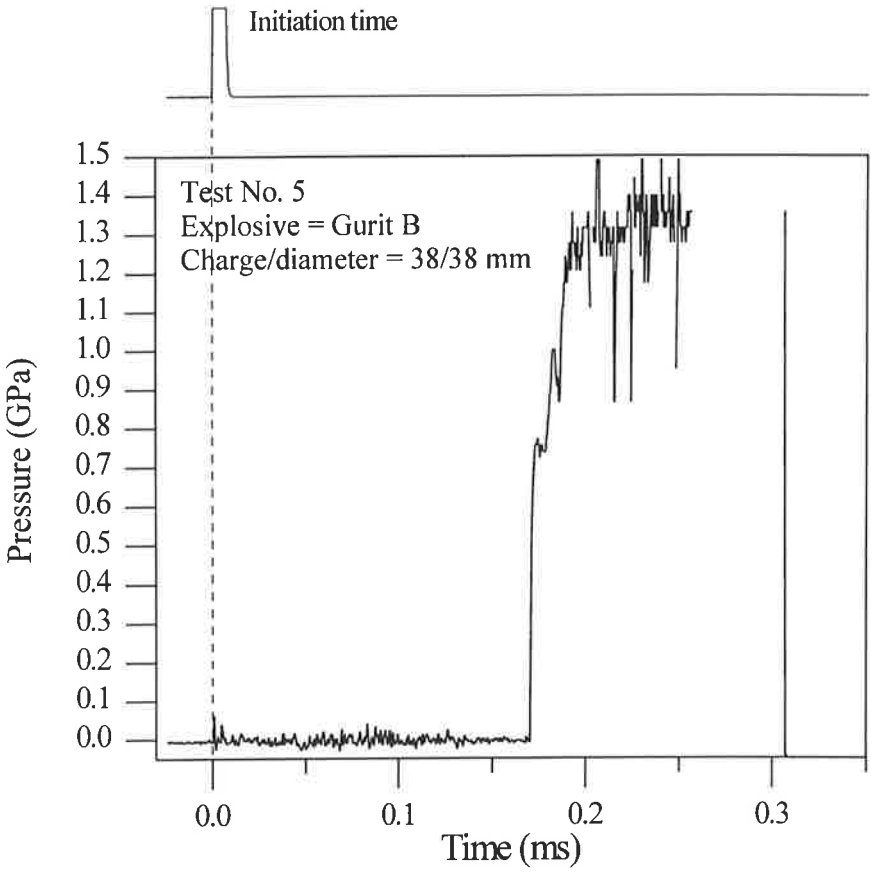

Fig. A8-a: Measured borehole pressure. Test No. 5. The LHM cup before and after the blast can be seen in Fig. A8-b.

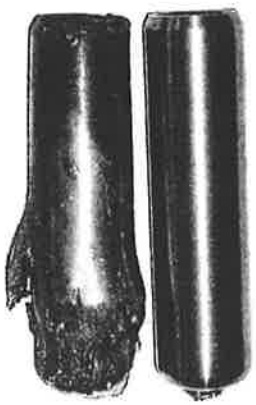

Fig. A8-b: The LHM cup before and after the blasting experiment in Test No. 5. The bottom part of the cup was diminished when it was squeezed into the cable hole by the pressure and the cup was burst by the pressure inside it.

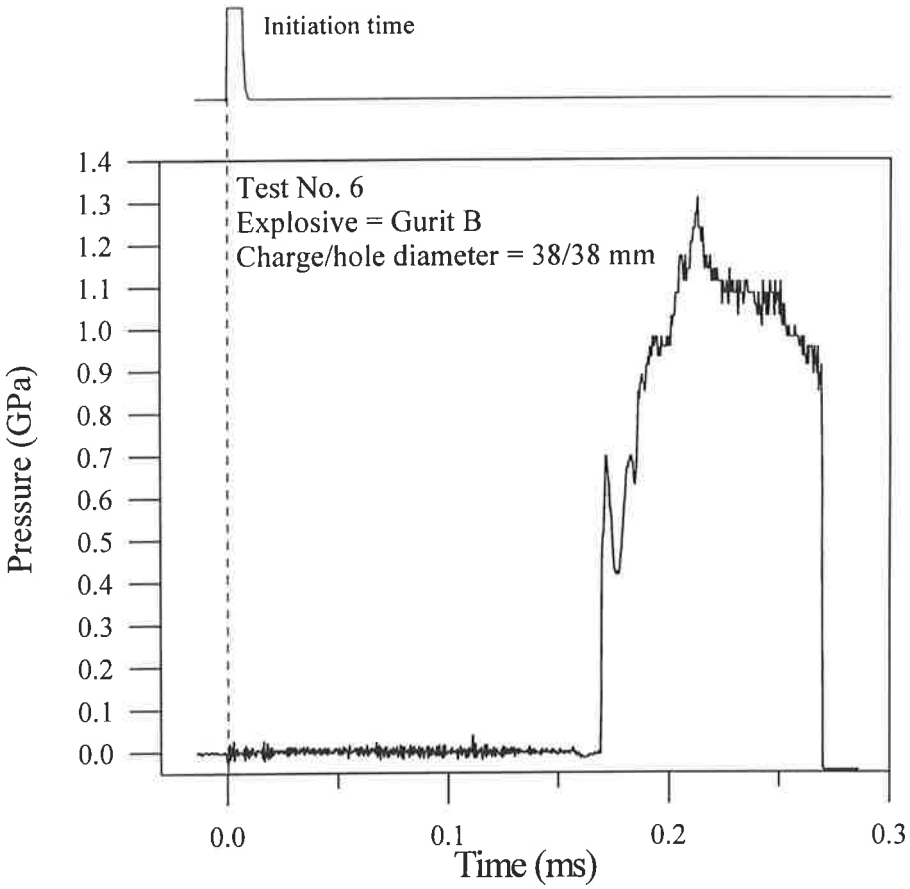

Fig. A9-a: Measured borehole pressure. Test No. 6. The LHM cup before and after the blast can be seen in Fig. A9-b.

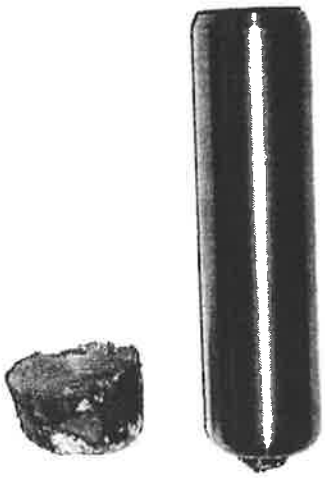

Fig. A9-b: The LHM cup before and after the blasting experiment in Test No. 6. Only the diminished bottom of the cup was recovered.

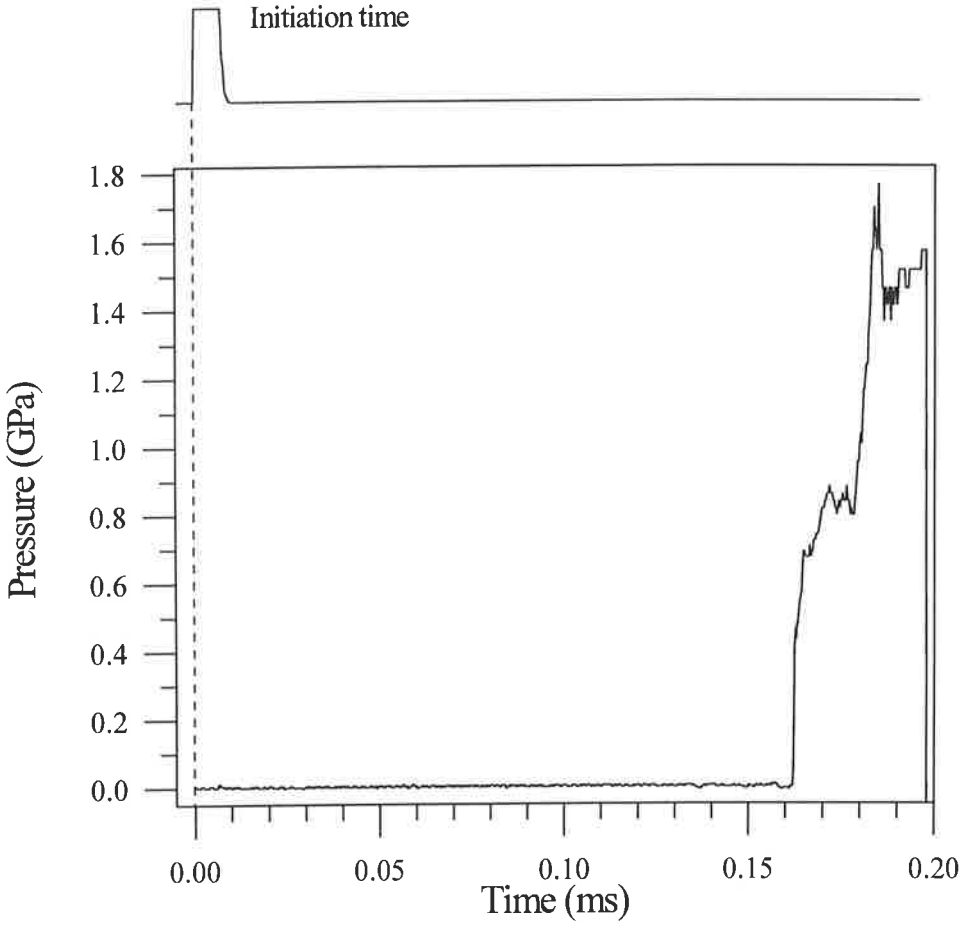

Fig. A10-a: Measured borehole pressure. Test No. 7. The LHM cup before and after the blast can be seen in Fig. A10-b.

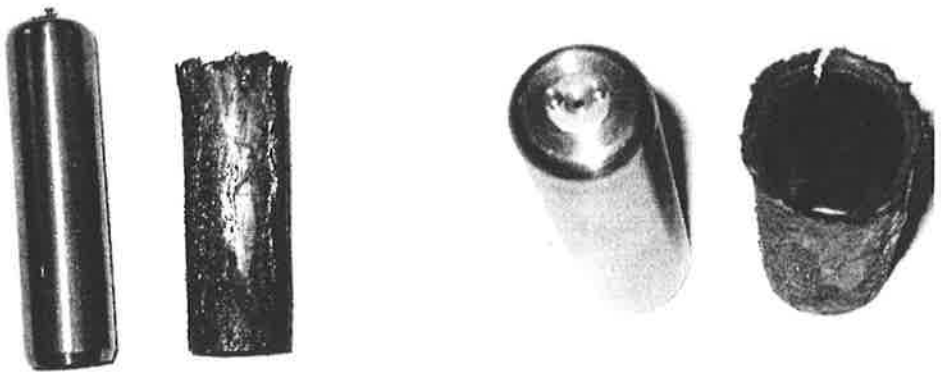

Fig. A10-b: The LHM cup before and after the blasting experiment in Test No. 7. The cup was swelled by the pressure inside and the bottom was blown away. Notes that in this shot, the LHM gage was mounted upside down on the top of the charge.

APPENDIX V: Illustration of the method to fill the gap between the LHM gage and the borehole wall with a chemical grouting material.

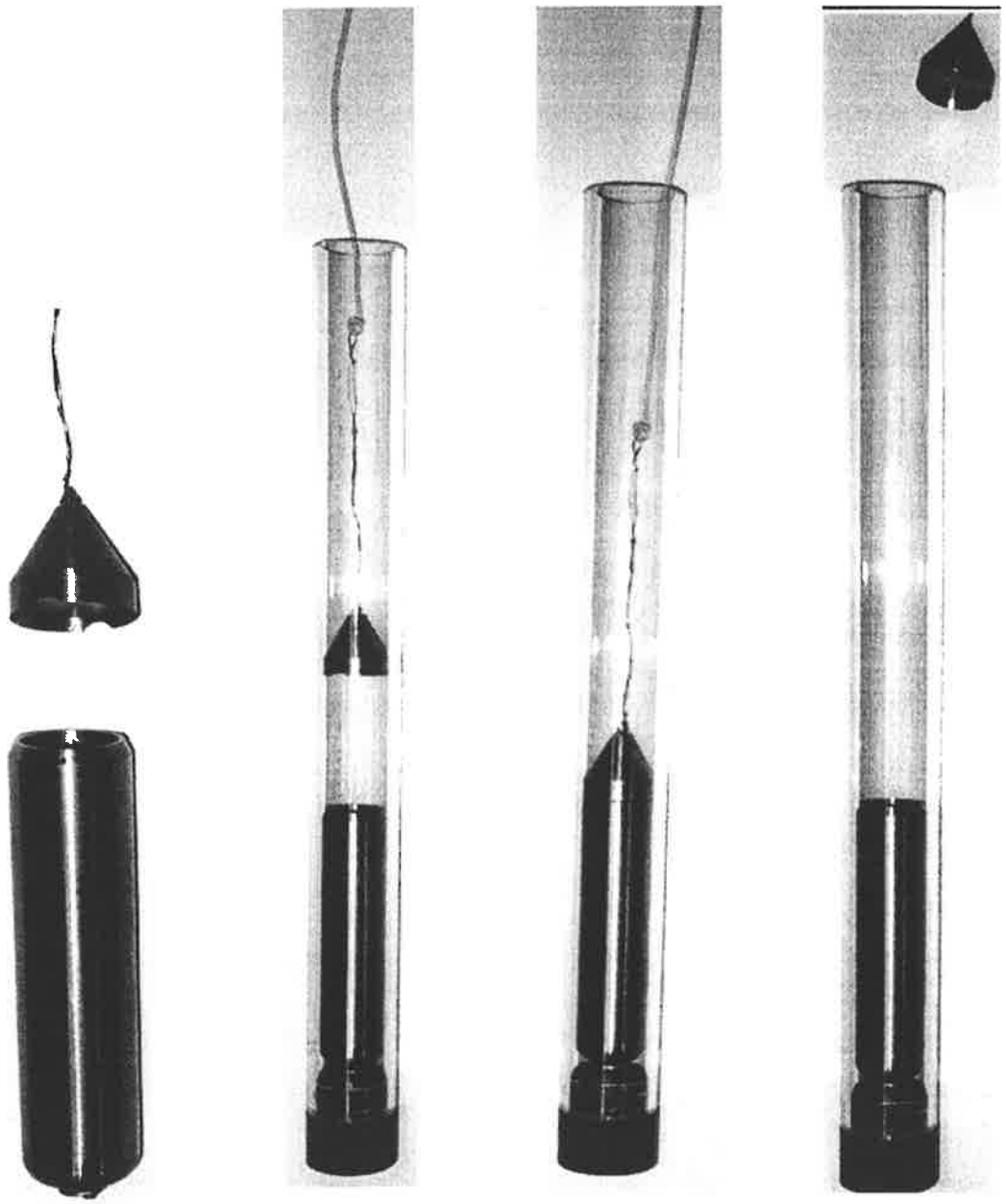

a) b) c) d)

Fig. A11: Method to seal the gap between the LHM gage and the borehole wall.
a: the top of the LHM cup is machined to fit a conical cap.
b: the conical cap is lowered on to the LHM cup and covers it.
c: Epoxy is poured into the hole, passes by the conical cap and fills the gap between the LHM cup and the borehole wall.
d: the conical cap is removed from the hole.